BOND PERFORMANCE OF CFRP/STEEL COMPOSITE AT ELEVATED TEMPERATURES

Egodawaththa Ralalage Kanishka Chandrathilaka

178012 R

Degree of Master of Science

Department of Civil Engineering

University of Moratuwa

Sri Lanka

October 2018

BOND PERFORMANCE OF CFRP/STEEL COMPOSITE AT ELEVATED TEMPERATURES

Egodawaththa Ralalage Kanishka Chandrathilaka

178012 R

Thesis submitted in partial fulfillment of the requirements for the degree Master of Science in Civil Engineering

Department of Civil Engineering

University of Moratuwa

Sri Lanka

October 2018

DECLARATION

I declare that this is my own work and this thesis does not incorporate without acknowledgement any material previously submitted for a Degree or Diploma in any other university or institute of higher learning and to the best of my knowledge and belief it does not contain any material previously published or written by another person except where the acknowledgement is made in the text.

Also, I hereby grant to University of Moratuwa the non-exclusive right to reproduce and distribute the thesis, in whole or in part in print, electronic or other medium. I retain the right to use this content in whole or part in future works (such as articles or books).

Signature: Date:

The above candidate has carried out research for the Masters under my supervision

Name of the supervisor: Dr. (Mrs.) J.C.P.H. Gamage

Signature of the supervisor: Date:

ACKNOWLEDGEMENT

Under the Research Project, I had the opportunity of gaining a very valuable experience of how to apply the theoretical knowledge gathered throughout the four years as an undergraduate to produce important findings for the well-being and development of the community.

There are number of persons whom I must pay my gratitude for their help towards the successful completion of the research project and report.

First, I am very grateful for the valuable guidance and encouragement given by my research supervisor, Dr. (Mrs.) J.C.P.H. Gamage, Senior lecturer in the Department of Civil Engineering, University of Moratuwa and my research chairperson Prof. P.B.R. Dissanayake, Senior professor in the Department of Civil Engineering, University of Peradeniya. Further I am thankful to senior professor, Prof. A.A.D.J. Perera for evaluating and giving us valuable instructions regarding the research findings we presented during the research progress presentations. Furthermore, I would like to appreciate the assistance of senior lecturer Dr. H.M.Y.C. Mallikarachchi on numerical modelling. It is highly appreciated the assistance of Dr. S. Fawzia, Senior lecturer in School of urban development, Qeensland University of technology, Australia over the support on publications.

Finally, I pay my appreciation to Mr. D.M.N.L. Dissanayaka, non-academic staff of Department of Civil Engineering, University of Moratuwa who helped us in experimental work.

Chandrathilaka E.R.K.
Department of Civil Engineering
University of Moratuwa
01.10.2018

ABSTRACT

Carbon Fibre Reinforced Polymer (CFRP) is being used as a retrofitting material for different structures such as, concrete and steel. Glass transition temperature (T_g) of the bond between CFRP and steel influences on the service and fire performance of strengthened members. A total of eighty-two CFRP/steel double strap joints were prepared and tested under elevated temperature. They were cured under a range of elevated temperature conditions in the control laboratory environment and in the open environment which is practically feasible in large civil engineering structures. The test results showed a similar trend of reductions in the bond strength, Poisson's ratio and Elastic modulus of CFRP/steel joint with the exposure to the elevated temperature. More than 50% reduction in the Poisson's ratio, elastic modulus and the bond strength was noted when the bond line temperature exceeds T_g + 15 ^{0}C, irrespective of the curing time and curing conditions. Initial elevated temperature curing also causes for shifting the curves in the right-skewed direction. A significant increase in T_g of bond was noted with 4 hours initial curing at 75 ^{0}C, i.e. T_g +20 ^{0}C.
Then a numerical model develops to predict the bond characteristics of CFRP/steel composites cured under different curing conditions and their behaviour at elevated temperatures. The measured material properties and their degradation with the temperature exposure were considered. The predicted bond performance was in a good agreement with the test results. The strain variation in the CFRP sheet was used to develop the bond shear stress-slip variations. Parametric studies were also conducted to evaluate the effects of bond line parameters on the bond shear stress-slip relationship at elevated temperature. The results indicate that the maximum bond shear stress of the joint lies in the range between 25 MPa and 28 MPa at ambient conditions, irrespective of the curing type. A rapid decrease in the maximum bond shear stress appears with exposure to the elevated temperature. Maximum shear stress reaches 10 MPa when the bond line temperature exceeds 90 ^{0}C. The elevated temperature curing, exposed temperature during service and the bond thickness notably affects on the bond slip behavior.

Key words: CFRP/steel bond, Glass transition temperature, Elevated temperature curing, elevated temperature testing, Fire, Bond characteristics, Bond stress-slip, Bond line properties

LIST OF PUBLICATIONS

International Journals

1. Mechanical characterization of CFRP/steel bond cured and tested at elevated temperature – Composite Structures – Published
2. Numerical modelling of bond shear stress slip behavior of CFRP/steel composites cured and tested at elevated temperature – Composite Structures – Under review
3. Effects of elevated temperature curing on glass transition temperature of steel/CFRP joint and pure epoxy adhesive – Electronic Journal of Structural Engineering (EJSE) – Under review

International Conferences

1. Bond slip models for corroded steel/CFRP double strap joints - 6th International Symposium on Advances in Civil and Environmental Engineering Practices for Sustainable Development (ACEPS-2018) – Published
2. Fire performance of CFRP strengthened steel I beams cured at elevated temperature - The 9th International Conference on Sustainable Built Environment 2018 (ICSBE) - Submitted

Contents

LIST OF FIGURES

Page

LIST OF TABLES

Page

LIST OF ABBREVIATIONS

Abbreviation	Description
CFRP	Carbon Fibre Reinforced Polymer
FE	Finite Element
UHM	Ultra High Modulus
HM	High Modulus
GP	General Purpose

LIST OF APPENDICES

Appendix	Description	Page
Appendix A	Publications	57
Appendix B	Experimental data (Spreadsheet, CD Attachment)	
Appendix C	Numerical analysis data (Spreadsheet, CD Attachment)	
Appendix D	Fire performance analysis (Spreadsheet, CD Attachment)	

1. INTRODUCTION

1.1 Research Background

The uses of steel for structural purposes can be witnessed in almost every country in the world. These uses of structural steel varied from simple roof truss to gigantic construction projects such as bridges and skyscrapers. However, one main drawback of use in structural steel is corrosion which will ultimately weaken the structure. Other than that, fatigue, insufficient design detailing, construction deficiencies, design errors, sub-standard materials, poor workmanship and lack of proper maintenance also lead to weaken the structure. In these cases, to retrofit the steel structure more feasible method is required apart from more conventional methods.

However, advanced composite materials have recently found their way into civil engineering infrastructure. With rising construction costs, engineers and owners are looking to these materials for a variety of applications. While not commonplace in current structural engineering practice, the benefits of advanced composites are rapidly becoming evident. The ability to design the material, coupled with high strength-to-weight ratio, allows engineers to maximize material usage for specific applications.

Carbon fibre reinforced polymer (CFRP) is one of the main composite materials that can use for the above purpose. In these cases CFRP will be used as a load transferring material from steel. Therefore, to transfer loads from one material to another, there has to be perfect bond performance between two materials. Therefore, the bond performance of steel/CFRP composite is crucial.

As the corrosion is the main drawback of use of structural steel, the bond performance of steel/CFRP composite is highly rely on the surface preparation of the corroded steel surface. However, there is a lack of knowledge on this matter, which is a crucial factor in steel/CFRP bond performance.

There is a lack of fundamental knowledge on the performance of CFRP/steel composites in elevated temperature, which will largely affect the bond performance of CFRP/steel bond in an event of fire. However, it was found that elevated temperature curing of CFRP/steel bond can increase the bond performance of CFRP/steel composites (Nguyen, T. et al., 2013). Therefore, elevated temperature curing can be used to increase the performance of steel/CFRP bond at elevated temperatures. The effects of elevated temperature curing on glass transition temperature (T_g) of bond also an area which require more attention.

The research presented in this thesis focuses on the above mentioned issues under surface preparation of corroded steel/CFRP bond and effects of elevated temperature curing on steel/CFRP bond performance at elevated temperatures.

1.2 Objective

The main objectives of this thesis is to evaluate the effects of elevated temperature curing of steel/CFRP bond in elevated environment temperature.

1.3 Methodology

First, a detailed literature review was carried out to investigate the steel/CFRP bond performance. Then experiments were carried out to evaluate the effective bond length. The results were used to evaluate steel/CFRP bond performance of bond cured and tested at elevated temperature. Then preliminary FEM was carried out on CFRP/steel bond performance using effective bond length data. Finally, numerical investigation was carried out to evaluate the steel/CFRP bond performance of bond tested and cured at elevated temperature.

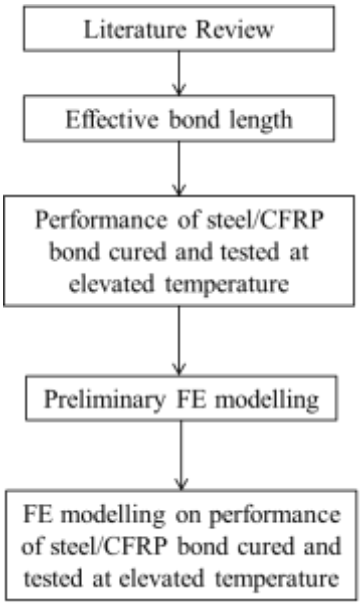

Figure 1.1 Flow Chart of Methodology

1.4 The Arrangement of the Thesis

In this report the research project has been presented with eight chapters. The first chapter contains the introduction, objectives and methodology of the research.

Second chapter contains the details of past research studies relevant to the proposed research title and the research gap.

Third chapter contains the experimental studies while the fourth chapter discusses the analysis of experimental results.

Then, the fifth chapter contains the preliminary numerical modeling and prediction of experimental results.

The sixth chapter contains numerical modeling on numerical modeling of steel/CFRP bond cured and tested at elevated temperature.

Final chapter contains the conclusions relevant to the research that have been done.

2. LITERATURE REVIEW

2.1 Introduction

Carbon Fiber Reinforced Polymer (CFRP) is being used as a retrofitting material for structural elements from past few decades significantly. The main advantage of the CFRP is the very high strength to weight ratio compared to other structural materials. Also the flexibility of raw CFRP sheets provide a great deal of easiness over applying the CFRP to the structural elements.

However, using of CFRP as a strengthening material on steel has been noticed as some distance behind compares to the use of CFRP to strengthen concrete and concrete base composite materials. The use of CFRP strengthening techniques on corroded steel has a vast untouched area compare to the above fact. Different techniques which were followed in different researches will be reviewed following by an assessment over a bond stress vs maximum shear stress model which can be used to understand the behavior of CFRP steel shear surface.

Curing condition of CFRP/epoxy/steel bond can affect the long term and short temp performances of the bond such as glass transition temperature (T_g), failure load, elastic modulus, durability, etc. Behavior of CFRP/steel bond under a fire will be also more relevant study which can affect the insulation cost of the bond.

2.3 CFRP as a strengthening material on steel

In the cases of using CFRP as a strengthening material for steel, it has shown more extraordinary results comparable to the concrete and other composite materials. Elchalakani, M. et al. (2017) have investigated the behavior of steel struts reinforced with CFRP sheets subjected to uniform axial compression with varying thickness of steel plate. Location and the number of CFRP sheets after strengthening with CFRP all the specimens had shown a great improvement in mechanical properties compare to un-strengthen steel specimens. It was calculated that the average increase in load carrying capacity after strengthening by CFRP was in the range between 256% and

452%. The maximum energy absorption and ductility increment was 259% and 107%, respectively.

CFRP strengthen steel had shown a very good resistance to fatigue loads. Colombi, P. and Fava, G. (2016) have discussed the fatigue crack growth of steel beams strengthen using CFRP in experimental and analytical basis. I-shape steel beams were used in the testing procedure with an average flange width of 64 mm, flange thickness of 6.3 mm, web thickness of 4.4 mm and total depth of 120 mm. CFRP was applied on the bottom of steel beam of 800 mm length to have an effective span of the beam to 1000 mm. It was found that using of CFRP in the beam has decreased the fatigue crack growth compared to un-strengthen steel. With use of two CFRP layers the overall fatigue capacity of beam was increased significantly.

Liu, M. and Dawood, M. (2017) have discussed about a reliability based analysis of double lap shear joints between steel and CFRP. Past experimental results were compared with the Hart-Smith model for bond strength prediction of thin adherents with using First Order Reliability Method (FORM) and Monte-Carlo Simulation (MCS) to analyses the co-relation of data. It was discovered that when considering the bond strength and reliability, adhesive's plastic shear strain capacity is the most influential material property. However, with large adhesive ductility may not help to higher resistant factor as the surface preparation. Premature adhesive failure can influence the resistant factors. Sand blasting the surface may increase the resisting factors of bonded steel CFRP joints than the angle grinding in surface preparation.

The in-situ strengthening techniques to retrofit deteriorated steel channel sections, size 1000 mm x 50 mm using CFRP were researched by Selvaraj, S. and Madhavan, M. (2016). The web and flange thickness were 5 mm and 7 mm, respectively with a total length of specimen of 1.4 m. Some specimens were subjected to bending and twisting failure with lateral torsional buckling due to the openness of the cross section. However, this can overcome by transforming the open channel section into a closed rectangular section. When using unidirectional CFRP fabric it would increase the flexural stiffness with a number of CFRP layers. However, when using bi-

directional CFRP fabric it would increase the torsional stiffness with a number of CFRP layers. So using of bi-directional CFRP fabric may improve the channel sections' resistance to lateral torsional buckling.

Elchalakani, M. (2016) has focused on the rehabilitation of corroded steel circular hollow sections(CHS) under quasi-static large The main observation of the test results was failure mode of the steel CHS, strength gain by the steel CHS due to CFRP application, effect of the severity of the corrosion deformation three-point bending and direct indentation tests. It was concluded that using CFRP can be used to increase the flexural and bearing strength of corroded steel CHS significantly. However, the percentage increase of the strength was mostly affected by the level of corrosion. Load carrying capacity of CHS can be increased by an average value of 97% using CFRP. Using of more number of CFRP sheets in circumferential and longitudinal direction, it may lead to increase the capacity 40% – 80% depending on trhe resulted surface profile due to corrosion.

Batuwitage, C. et al. (2017) have focused on bond characteristics and environmental durability of degraded CFRP strengthened steel plate double strap joints. When the corrosion increases the failure mode has shifted from CFRP fiber rupture to steel adhesive debonding due to degradation of material properties at the interface between adhesive and steel. However, it was found that the lower shear strength leads to reduction in bond strength of bonded joints in corroded steel samples.

2.2 Different loading conditions used in testing

Loading rate and loading condition can affect the final results of a test. With different loading rates the results such as ultimate strength, final deformation, shear stress vs strain graphs can be varied significantly. Therefore, it is important to use a loading rate, which can simulate good agreement between test and real life situation.

Al-mosawe, A. et.al. (2016) have discussed about the application of genetic programming (GP) to predict the bond strength of CFRP-steel double strap joints

subjected to direct tension load in two different loading conditions, 2mm/min quasi-static loading and 201x103 mm/min – 300x103 mm/min high loading rates. It was found that high loading rates of specimens have led to high bond strengths compare to the low quasi-static loading rates when all the other factors are constant.

Yu, Q. Q. et al. (2016) have investigated more intensive fatigue loading conditions. It was used the specimen sizes as described in the literature with 450x50 mm steel plates with 8mm thickness and CFRP laminate on a single side with 50mm and 25mm width. A fatigue load was applied to the plate as a tensile load with 10Hz and stress ratio of 0.4. It was observed that fatigue loading conditions have adversely affected CFRP bond compared to normal static loading conditions.

2.3 Finite Element modelling of CFRP steel double strap joints

In general, numerical modeling provides convenient and fast solutions for an investigated phenomenon. However, validation of the model is important before any predictions.

Ghaemdoust, M. R. et.al. (2016) have discussed about the structural behavior of the steel square hollow section (SHS) compression members having initial horizontal or vertical deficiencies which were strengthened using CFRP. A total of thirteen specimens was used in experiments with one control specimen. Three-dimensional modeling and non-linear static analysis were carried out using a FEM software. The steel hollow sections were with 90 mm x 90 mm dimensions with 3 mm in thickness and 270 mm in length. Position and dimensions of the deficiencies were changed in the 12 specimens which were tested. Total 8 specimens with CFRP layers and 4 without CFRP layers were used in testing. In the numerical modeling tetrahedron quadratic (10 nodes) elements were used for steel section and hex quadratic (20 nodes) elements were used for adhesive and CFRP. High correlation between numerical and experimental results were observed with values between 1.01 to 1.04.

The strengthening of steel plates with an opening using CFRP under fatigue tensile loading was discussed by Wang, Z. et.al. (2017). Experimental and finite element analysis was carried out in the research. In the numerical analysis, commercially available FEM software package was used. Steel plates were modeled using SOLID 95 elements with 20 nodes and three degrees of freedom per node, while CFRP layer was modeled with SHELL 91 element with 6 degrees of freedom at each node. Only ¼ of the actual dimensions were considered in modeling considering the symmetry. It was found that applying CFRP on steel plates with openings can increase its fatigue life by 20% to 60% in both numerical and experimental results.

Al-zubaidy, H. et.al. (2013) have presented a numerical simulation for steel- CFRP double strap joint with one and three CFRP layers per side with quasi-static and dynamic tensile loading. Three dynamic loading speeds were used 3.35 m/s, 4.43 m/s and 5 m/s. Steel specimens were used with dimensions 210 mm x 50 mm x 5 mm. Bond length was varied in the testing process of 160 specimens. Commercially available FEM software was used in the finite element modeling and 8-node three-dimensional cohesive element for adhesive layers, 8- node three-dimensional reduced integration first order hourglass control element for steel plate and 8- node quadrilateral in-plane general- purpose continuum shell for CFRP patch were used to develop the model. It was observed a large discrepancy between numerical and tested results with increased number of CFRP layers even though reliable results were noted from the model which contains a single layer of CFRP.

However, it was also possible to model the adhesive layer in shell elements. Yue, Q. et al. (2016) have discussed the performance of CFRP reinforced steel girders with the aid of experiments and numerical modelling. Numerical modeling was carried out following the experiment using a finite element software. ‘Solid-shell” elements were used in the modeling of CFRP reinforced steel girders, while “shell” elements were used to model the adhesive and CFRP layers.

Size of elements in the FE model is crucial as it governs the accuracy of the FE model. With smaller size elements the accuracy may increase with an increase of

solving time and solving resources, which will be a disadvantage. Therefore, using of smaller elements in crucial places of the model may increase the accuracy of the FE model without increasing the solving time considerably (Yue, Q. et al. (2016) and Al-zubaidy, H. et.al. (2013)).

2.4 Bond slip vs maximum shear stress modal

Most common criteria which was adopted to determine the bond performance is the ultimate bond strength. However, this performance can be changed with the geometry of the specimen and other loading and testing conditions. Therefore, it is required to have a more reliable method to evaluate the performance of the bond without depending on the geometry of the specimen. Local bond -slip model follows an independent relationship of geometric conditions and it can evaluate the bond performance more universally compared to the bond strength itself (Focacci, F et.al. (2000) and Lu, X.Z. et.al. (2005))..

This bond slip model can be used to determine the bond performance of composites like CFRP strengthen concrete. Dong, K. and Hu, K. (2016) has discussed the effect of high temperatures on CFRP to concrete joints. Two parameter bond-slip relationship was formed to present the behavior of CFRP concrete joint in high temperatures. It was observed that in high temperatures the bond properties are closely related to the temperature difference between the service temperature and glass transition temperature for the CFRP to concrete joints.

Fawzia, S. et.al. (2010) has investigated the bond behavior of using experimental and numerical analysis on CFRP strengthened steel double strap joints under tension. The bi-linear bond slip model was used as the approximation of CFRP plate.

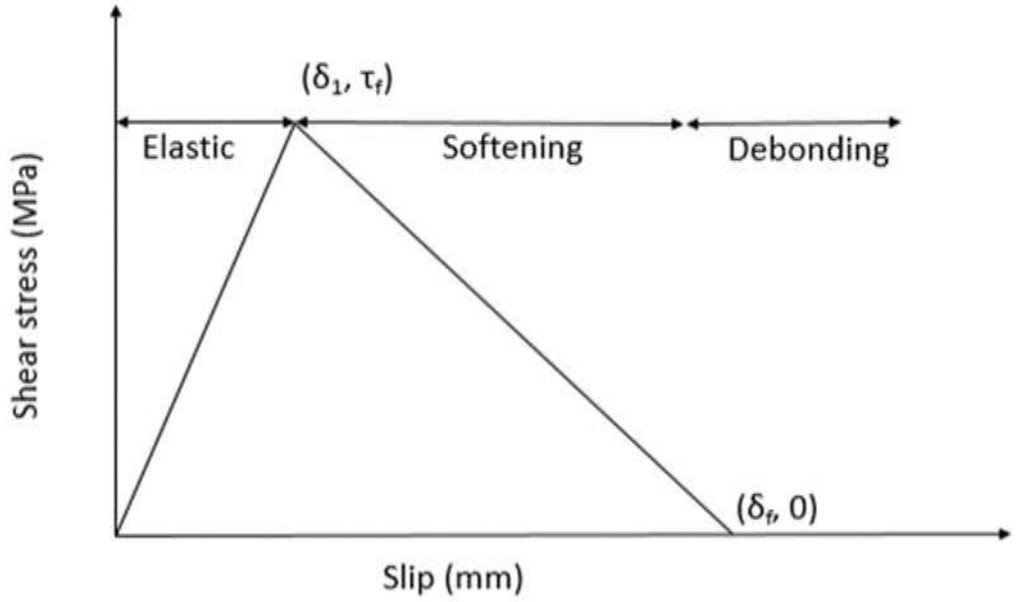

Figure 2.1 Bi-linear shears tress vs bond slip model

The bond slip relationship was proposed to the three types of adhesives on parametric study area. It was observed the shear stress tends to decrease from the loaded edge to the distance away from the joint. However, after the effective bond length the bond slip model could not be used. Maximum slip of the adhesive was directly influenced by the assumed peak strain in the stress strain plot. However, it did not effect on the maximum shear stress and initial slip values. Initial slip and maximum slip increased as the adhesive layer thickness increases.

2.5 Glass Transition temperature

The glass transition temperature (T_g) is an important parameter, indicative of thermal behaviour of a material. In an epoxy glass transition temperature determines the region where the polymer transitions from a hard, glassy material to a soft, rubbery material. If this so called epoxy being used for a structural purpose, such as an adhesive, the degrading of mechanical properties in adhesive can cause a failure in the structure (Wang, R. et.al. (2011)).

2.5.1 Effects of micro structure of epoxy and polymers on glass transition temperature

Glass transition temperature is the macro-manifestation of polymer chain's flexibility. If the rigidity of polymer chain can be increased, then the glass transition temperature of the epoxy or polymer will be increased (Wang et.al. (2011)). Therefore, with altering the micro structure of the polymer chains in epoxy and polymers the glass transition temperature can be altered.

In the polymers, glass transition temperatures can be influenced by liquids. By separating the chains of the polymer to increase the general mobility of polymer chains, the glass transition temperature can be altered. However, the liquid should be compatible with the polymer. Most of the time, addition of compatible liquids may reduce the glass transition temperature of polymers by a value up to 1000C. Cross linking of polymers with other materials helps to reduce the segmental mobility between polymer chains. Due to this effect of cross linking glass transition temperature of polymers can be increased (Gilbert, M. (2017)).

In the epoxies glass transition temperature will be mostly affected by curing temperature. In an event of curing temperature is less than the average glass transition temperature of epoxy, glass transition temperature will be low compare to the curing temperature above the glass transition temperature. In high curing temperatures the mobility of the molecules is affected and it will increase the ability to resist high temperature. Therefore, high temperature will increase the glass transition temperature while improving other mechanical properties of the epoxy (Carbas, R. J. C. et.al. (2014)).

2.5.2 Measurement of glass transition temperature

Three main methods can be found to measure the glass transition temperature of a polymer (Carbas, R. J. C. et.al. (2014), Rudin, A. and Choi, P. (2013)).

- DCS – differential scanning calorimetry, measure the energy necessary to establish nearly zero temperature difference between a sample and an inert reference material.
- TMA – thermos-mechanical analysis, measure a physical response as a function of a time in a given temperature or at a linear heating rate
- DMA – dynamic mechanical analysis, measure the viscoelastic response of a material as a function of a time in a given temperature or at a linear heating rate

2.5.3 Effects of curing conditions on glass transition temperature (T_g)

Kotynia, R. et.al. (2017) has investigated the effect of variable curing conditions on commercially available epoxy adhesives for structural strengthening with externally bonded and near surface mounted FRP. Total number of eight series of adhesive specimens were tested with different curing conditions. Four numbers of specimens were cured on 85 ^{0}C temperature for 25 mins while the other four specimens were cured on 85 ^{0}C temperature for 35 mins. Before the testing cooling time of 10, 20 and 30 mins were allowed just after the curing. DSC (Different Scanning Calorimetry) method was used to determine the glass transition temperature of the epoxy adhesive with a heating rate of 10 ^{0}C/min. With increasing the curing time from 25 mins to 35 mins the shear strength of the joints was increased significantly. On the other hand, for the glass transition temperature, it was not observed any influence due to the increase of the curing time.

Carbas, R. J. C. et.al. (2014) has discussed about the influence of curing temperature on the physical and mechanical properties of three structural adhesives such as glass transition temperature (T_g), Young's modulus and strength. By using dynamic mechanical analysis (DMA) to measure the T_g value. Areldite 2011, Areldite AV 138M and Sikadur -30 LP were used in testing with various curing temperatures from 230C to 1400C. The initial curing stage was performed in those different temperatures for 30 mins and 120 mins ad post curing stage was performed at room temperature for 2 weeks. It was observed that T_g, stiffness and strength vary as a function of the cure temperature of the epoxy adhesive. More precisely, when specimens were cured below the T_{cure} the T_g, strength and stiffness increase as the

curing temperature increases. When the specimens were cured below the T_{cure} the T_g, strength and stiffness increase as the curing temperature decreases.

Zhang, Y. et.at. (2014) has discussed about the long term behavior of adhesives subjected to aggressive environments. It was discussed the fact that liquid absorption behavior of epoxy adhesives and glass transition temperature (T_g) in two different solvents and two different temperatures. Two types of epoxy adhesives were used in testing, AV119 and 2014. Adhesive AV119 is one-part paste epoxy with good heat and chemical resistance, which needs to be heat cured while Adhesive 2014 is room temperature curing two-component paste. Specimens were cured in 60 ^{0}C and room temperature with submerged in toluene and water. When it was compared the weight gain of the specimens' high temperature immersions were shown higher value compared to the low temperature immersions. It was found that the liquid uptake has influenced the T_g value significantly. T_g become lower in case of drying process in unexposed adhesives. It was discovered when specimens were heated above the T_g value for even a short time, it significantly influenced the liquid intake of the specimens.

2.5.4 Effects of curing condition on other mechanical properties on CFRP joints

Curing condition effects not only the T_g, but the mechanical properties of the joint also. Nguyen, T. et al. (2013) have discussed the behavior of steel and the CFRP double strap joint with different curing conditions under combined loading, cyclic temperature and humidity. Two curing conditions were used in the test series, room temperature curing for 14 days and 120 ^{0}C curing for one hour following 14 days' room temperature curing. Curing in higher temperature has not improved the strength of steel – CFRP joints which were tested at room temperature. However, it was found that testing on elevated temperature may increase the strength.

2.5.5 Effects of high temperatures on mechanical properties of CFRP steel joints

In the high temperature testing the mechanical properties of the bond can be affected, especially the bond strength. Nguyen, T. et al. (2011) have observed the mechanical performance of steel CFRP adhesively bonded double strap joints at elevated temperatures. In the experiment, it was discussed the temperature effect on joint effective bond length, temperature effect on joint stiffness, temperature effect on joint strength, temperature effect on joint failure mode. Effective bond length has increased with the temperature in experimental results. However, joint stiffness has decreased with the temperature. In lower temperatures, joint has failed due to CFRP delamination while in higher temperatures failure was happen due to cohesive failure. Due to the shear strength degradation of adhesive with high temperature the joint ultimate load capacity has decreased. Reduction of the ultimate joint capacity is high when the bond length is less than the effective bond length.

Agarwal, A. et.al. (2016) have observed the effect of thermo-mechanical loading in wet and dry conditions on steel CFRP single lap joints with the aid of experimental investigation. In the wet conditions the failure mode was debonding failure at the interface between steel and adhesive. In the dry conditions, failure mode was shifted to delamination failure. In the thermal cycling the moisture content is critical as it can reduce the bond strength of the steel CFRP joint.

2.6 Summery

The research on strengthening technologies related to adhesive bonding of CFRP composites onto structural steel members at elevated temperatures is still in its infancy. There is a need to improve effective curing techniques for steel structures bonded by CFRP sheet to perform better at elevated temperatures. The following issues will be covered by this research.

- Effective bond lengths for steel/CFRP bond
- Effects of curing methods on strength of CFRP/steel bond at elevated temperature

- Effects of curing temperature and period on strength of CFRP/steel bond at elevated temperature
- Effects of curing condition on adhesive properties at elevated temperature
- Effects of curing condition on bond behaviour of CFRP/steel bond at elevated temperature

3. TEST PROGRAMME

3.1 Specimen preparation

Appropriate preparation of the bonding surfaces in any application involving adhesives is of paramount concern. The strength of the adhesive bond is directly proportional to the quality of the surfaces preparation. All surface must be cleaned from all the impurities. A surface with small irregularities provides additional surface area for the adhesive to bond along with some mechanical resistance to shear at the bond interface. Conversely, a surface that is smooth or one that has a slick finish does not produce nearly as strong a bond because shear cracks can quickly propagate un-impinged along the length of the bond. Therefore, surface preparation of steel was done with sand blasting the steel surface to clear the surface from all forms of rusts and to make the surface with more irregularities. However, a thin layer of corrosion resistance epoxy was applied on the prepared steel surface to prevent forming any rust after the surface preparation.

Then two steel plates with dimensions 162 mm x 38 mm x 5mm were held in a horizontal position on a leveled surface and adhesive was applied on the surface of cleaned steel plates over the bond length. Then a layer of CFRP sheet which was cut into perfect dimensions of the bond length was placed on top of the adhesive. The sample was ribbed rolled to squeeze out excess adhesives. The dimensions of the steel plates were selected as used by Sabrina et al. (2010).

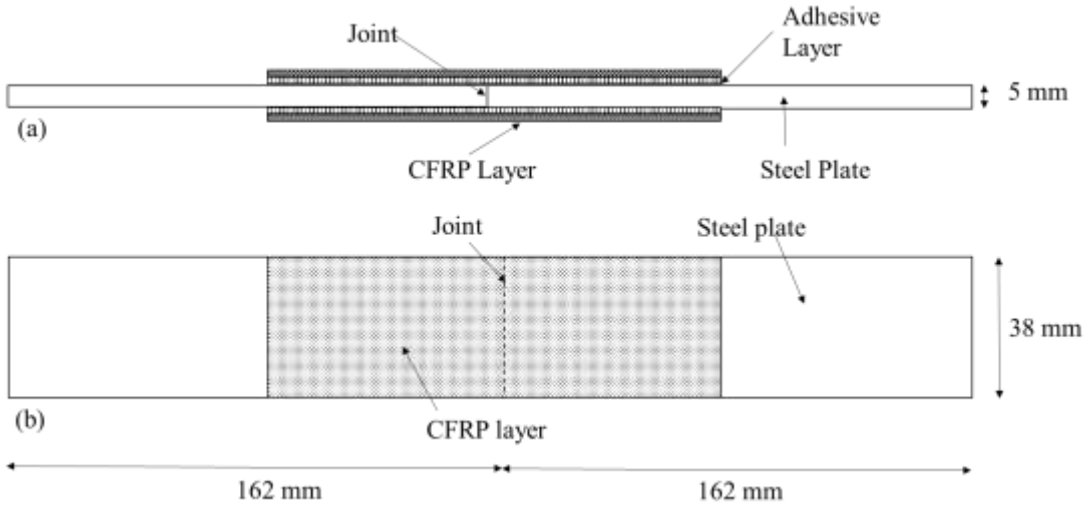

Figure 3.1 (a) Side View (b) Plan View of a Schematic diagram of the double strap joint

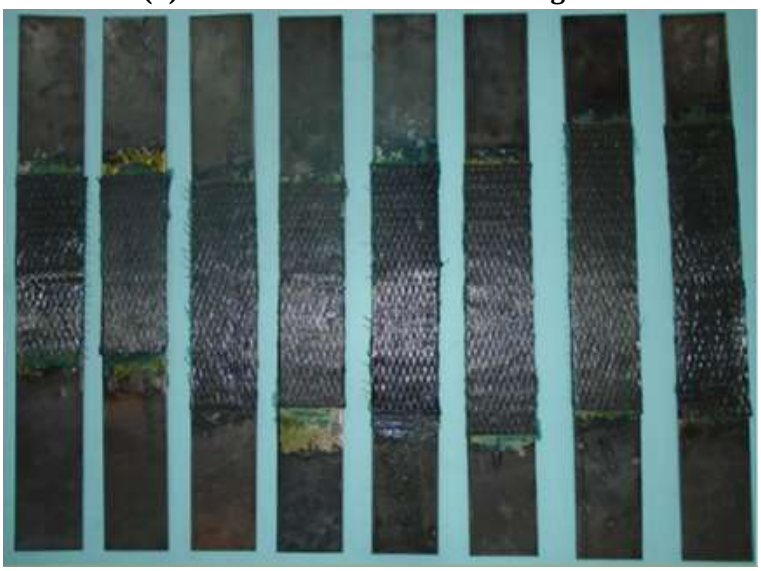

Figure 3.2 Prepared samples

3.2 Effective bond length

To find the effective bond length, fourteen numbers of double strap joints were prepared with the varying bond lengths between 40 mm to 120 mm. According to the results obtained, the effective bond length was identified to be 110 mm. All the specimens were kept to cure for at least 7 days. Bond strength was evaluated by testing the prepared samples in tension using a 1000 kN testing machine and a transient load were applied in the rate of 2 mm/min. Strain readings of the samples were measured using strain gauges.

3.3 Surface preparation method on different corrosion levels

This test series was consisted of 32 double strap joint specimens. The samples were prepared by taking into account two surface preparation levels and this was obtained by grinding away the rust layers in two different methods (Method 01, and Method 02). The curing and testing of these 32 samples were same as in section 3.2. Surface roughness parameters of the corroded steel surfaces were determined using the SEM (Scanning Electron Microscopic) images taken for each level of corrosion.

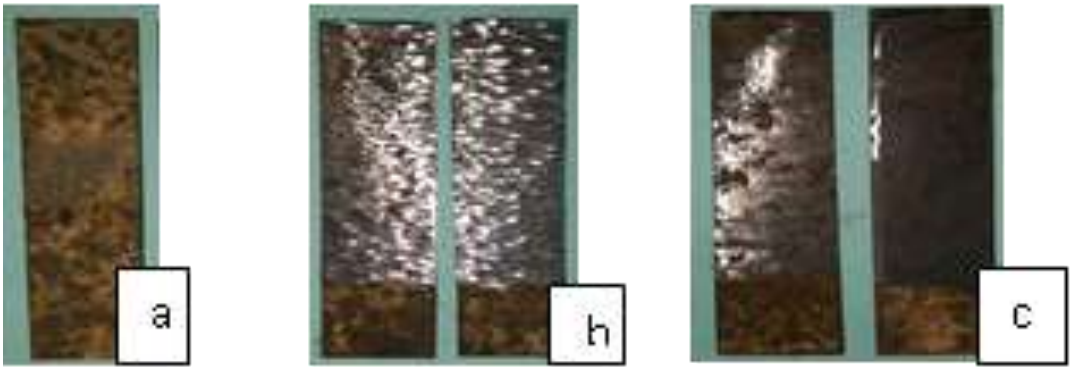

Figure 3.3 Steel plates: (a) Before grinding (b) Fully grinded (Method 01) (c) Partially grinded (Method 02)

3.4 Different curing conditions

Bond length one side of the double strap joint was maintained at 140 mm while the other side was maintained at 150 mm to maintain effective bond length as described in section 3.2. Type K thermocouples with 1 mm diameter was installed in the middle of the bond line to measure the temperature reading during the curing process as well as for the testing under elevated temperature. All thermocouples were calibrated before use.

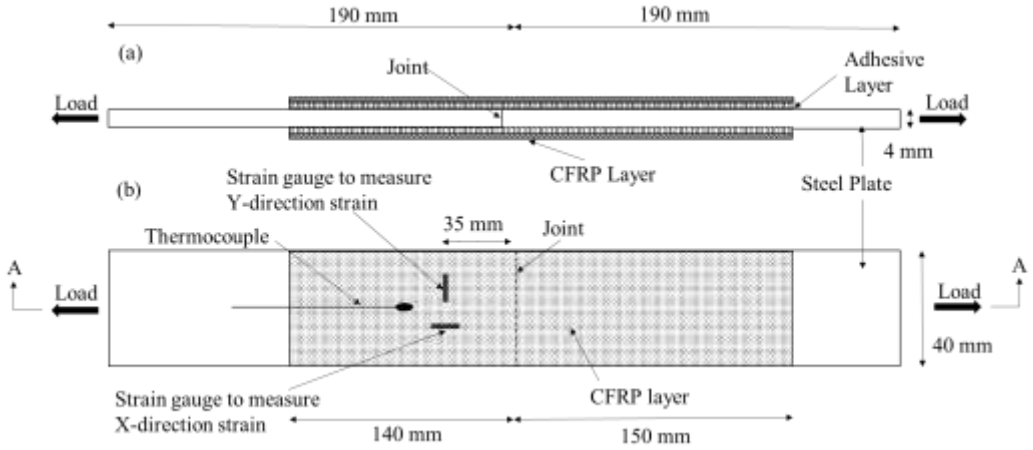

Figure 3.4 Schematic diagram of a double strap joint; (a) view A-A (b) plan view

Figure 3.5 Specimen samples after thermos-couple installation

In this test programme, five elevated temperature initial curing conditions were considered [Table 3.1]. In the elevated temperature curing, one of the series was cured using an oven, while other series were cured using a system of halogen floodlights with 1000 W capacity, which is a practically feasible method. All the specimens were kept under ambient temperature (30 ^{0}C) for 7 days after the initial elevated temperature curing at considered temperature levels for the relevant period. While curing using the floodlights, bond line temperature could maintain at $\pm$5 ^{0}C margin from the desired curing temperature. Figure. 3.6 shows the details of the both curing systems.

Table 3.1 Curing configuration

Specimen group	Elevated temperature Curing conditions			Total nos. of specimens
	Curing temperature (^{0}C)	Curing method	Initial curing time (hours)	
A/30-1	Ambient	Ambient	N/A	12
OH1/O-75-1	75	Oven	1	14
FH1/75-1	75$\pm$5	Floodlights	1	14
FL1/55-1	55$\pm$5	Floodlights	1	14
FH2/75-2	75$\pm$5	Floodlights	2	14
FH4/75-4	75$\pm$5	Floodlights	4	14

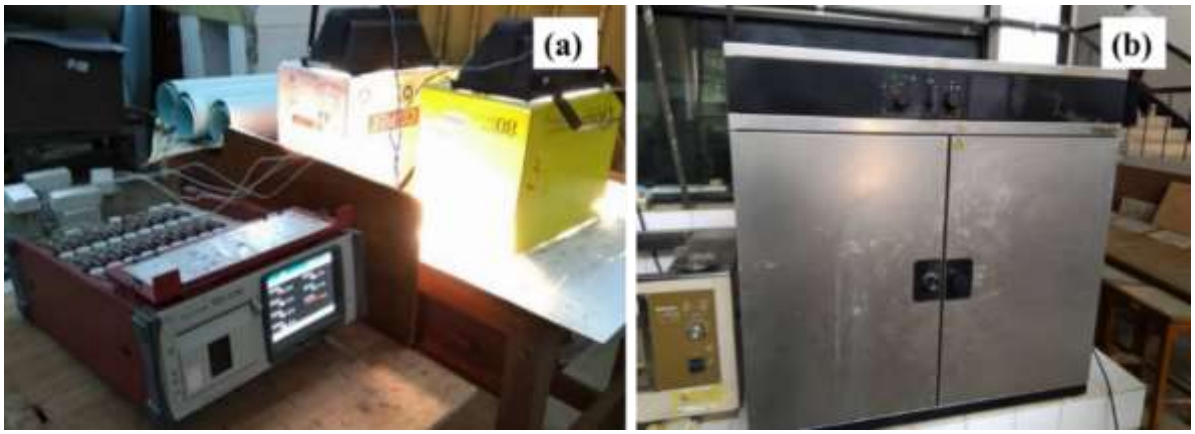

Figure 3.6 Elevated temperature curing using (a) halogen floodlights (b) standard oven

In the testing, the environmental temperature was raised till the bond line temperature reaches the required temperature level. Then the specimen was kept at the same temperature for 10 minutes till the bond line temperature becomes stable and uniform as predicted. The transient tensile load was applied to the specimens by maintaining the saturated temperatures at bond line as 30 ^{0}C (ambient temperature), 50 ^{0}C, 60 ^{0}C, 70 ^{0}C, 80 ^{0}C, 90 ^{0}C and 100 ^{0}C. The universal testing machine with 1000 kN capacity was used to apply the tension on the double strap joints [Figure 3.7].

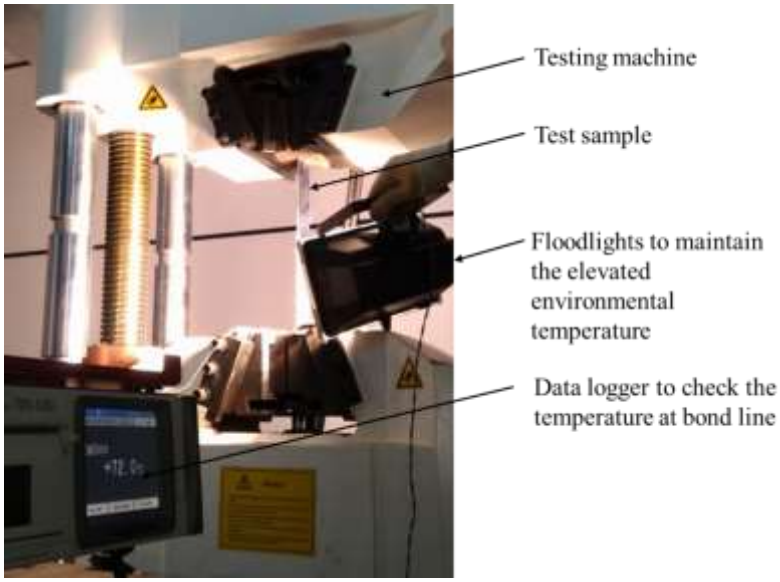

Figure 3.7 Test setup

4. MECHANICAL CHARACTERIZATION OF CFRP/STEEL BOND CURED AND TESTED AT ELEVATED TEMPERATURE

4.1 Test results

4.1.1 Failure load and mechanisms

The measured failure loads are listed in Table 4.1. Elevated temperature curing at temperatures slightly higher (75 ^{0}C) than the glass transition temperature (55^{0}C) of polymer adhesive (ARELDITE 420 A/B) showed increased strength than the samples cured at temperature lower (55 ^{0}C) than the T_g of epoxy adhesive. Mobility of polymer particles increases around the T_g of polymeric matrix (Gilbert, M. (2017)). This increased mobility may cause for proper rearrangement of polymer molecules during the initial curing stage, which result in the highest bond strength. When the specimens expose to the temperature near the T_g, the strength of all the samples had decreased, irrespective from the curing condition. A considerable strength reduction (70%) was noted when the bond line temperature reaches T_g + 40 ^{0}C. This may due to the weaken load transfer ability of CFRP/steel joint due to the softening of epoxy adhesive bond. Similar behaviour was also noted from the concrete/epoxy/CFRP joints (Gamage, et al. (2016), Gamage et al. (2007), Gamage et al. (2006)).

Table 4.1 Average failure load

		Specimen group					
		30-1	O-75-1	75-1	55-1	75-2	75-4
Bond line temperature at failure (^{0}C)	30	36.83	38.63	38.6	37.15	41.35	40.05
	50	33.4	35.62	37.6	34.43	35.95	37.8
	60	26.05	26.2	33.65	31.9	30.4	33.6
	70	21.18	25	28.05	23.83	27.6	31.13
	80	15.5	21.73	23.55	19.45	24.23	27.6
	90	15.63	13.83	16.03	13.15	17	16.7
	100		9.1	13.45	14.45	15.65	15.05

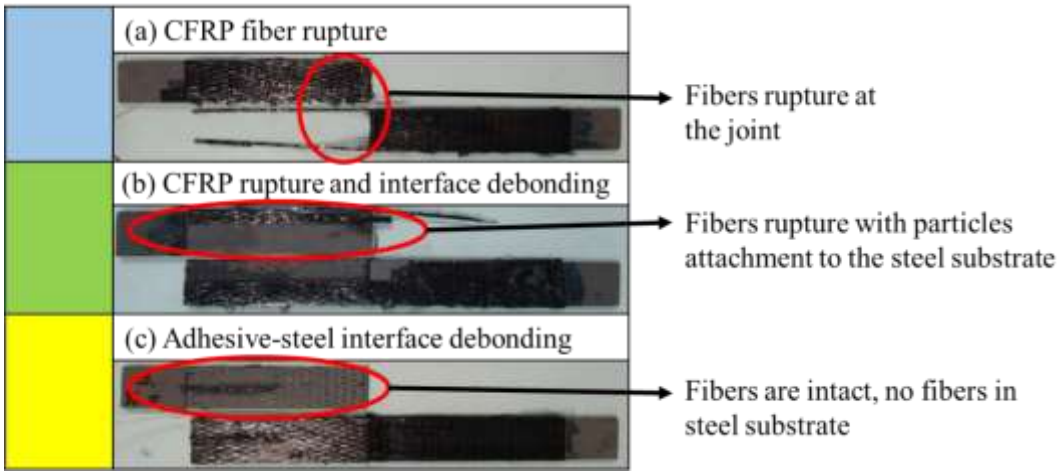

Figure 4.1 Failure modes

Three major failure modes were identified during testing: (a) CFRP fiber rupture, (b) Adhesive-steel interface debonding and (c) mix failure mode (CFRP fiber rupture and adhesive steel interface debonding) as shown in Figure. 4.1. CFRP fiber rupture failure mode was observed in the samples which were tested at 30 ^{0}C temperature, i.e. at environmental temperature. This provides evidence for a sound bond between CFRP and steel in the operating environment. Adhesive-steel interface debonding failure mode was observed only in the specimens which were tested at temperatures greater than 60 ^{0}C. This may due to the fact that softening of polymeric adhesive bond when it reaches its T_g. In the specimens failed due to a mix failure of CFRP fiber rupture and adhesive steel interface debonding, tested temperature was less than 80 ^{0}C [< (T_g + 25 ^{0}C)]. When the tested bond line temperatures were less than 60 ^{0}C [< (T_g + 5^{0}C)], specimens were tending to fail due to a CFRP fiber rupture. This indicates the lesser mobility of polymer particles when the bond line temperature is less than T_g result in a sound bond between CFRP and steel. Gamage et. al. (2007) noted the similar behaviour in CFRP/concrete composites when the joint exposes to the elevated temperature.

4.1.2 Effects of curing temperature on bond strength

Figure. 4.2 shows the strength of CFRP/steel joint when the bond line is exposed to the different temperature levels. These specimens were cured at two levels of elevated temperatures (55 ^{0}C and 75 ^{0}C) for one hour using halogen floodlight

system, before fully cured under the environmental temperature. These three graphs show a similar trend of degrading material properties which can be seen in polymeric adhesive bonds (Wang et al. (2011)).

The strength reductions when the composite is exposed to different temperatures have decreased with elevated temperature curing. This implies the evidence for increased glass transition temperature with the initial curing temperature. Increased T_g may cause for more stable bond even though it exposes to the elevated temperature. When the bond line temperature exceeds 90 ^{0}C, almost similar behaviour can be seen from all specimens irrespective from the curing conditions. On average, 70% strength reduction was noted when the bond line temperature becomes 100 ^{0}C. This shows the evidence for softening of bond when it exceeds the temperature beyond T_g + 40 ^{0}C. Nguyen et al. (2013) has observed the same effect of curing temperature as it did not improve the strength of double strap joints at ambient temperature (30 ^{0}C).

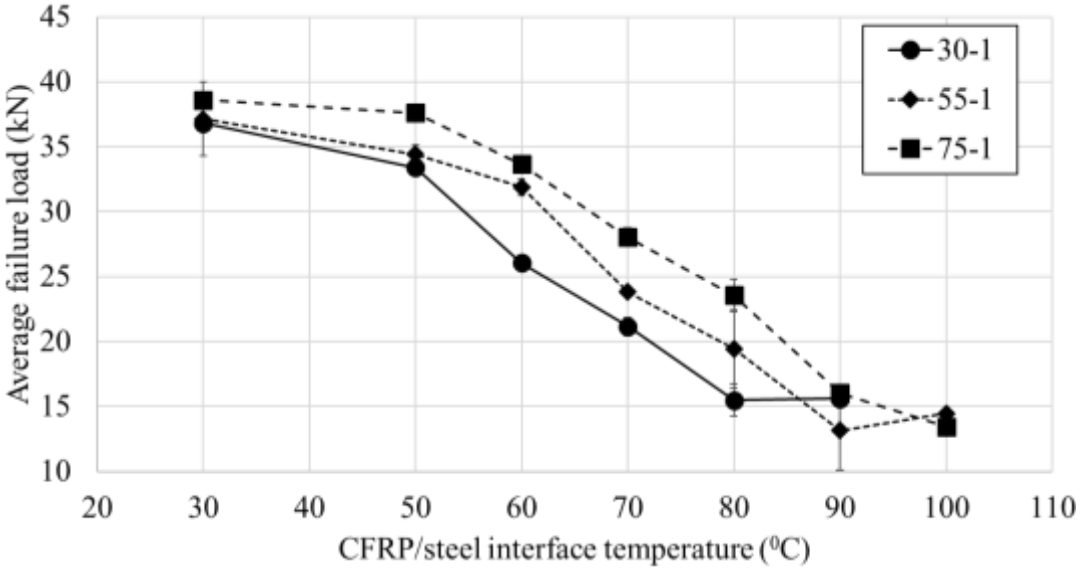

Figure 4.2Effects of curing temperature on average failure load

4.1.3 Glass transition temperature of CFRP/epoxy/steel bond

Glass transition temperature (T_g) for the double strap joints were calculated as shown in Figure. 4.3 for the samples which exposed to the different curing conditions. The definition used by Gamage et. al. (2016) was used to define the T_g. It

is found that the T_g of the CFRP/epoxy/steel bond cured under ambient condition is about 50 ^{0}C. This is 9% lower than the T_g of epoxy adhesive (ARELDITE 420 A/B) cured under the same conditions. This provides the importance of identifying T_g of bond rather than relying on the T_g of adhesive component.

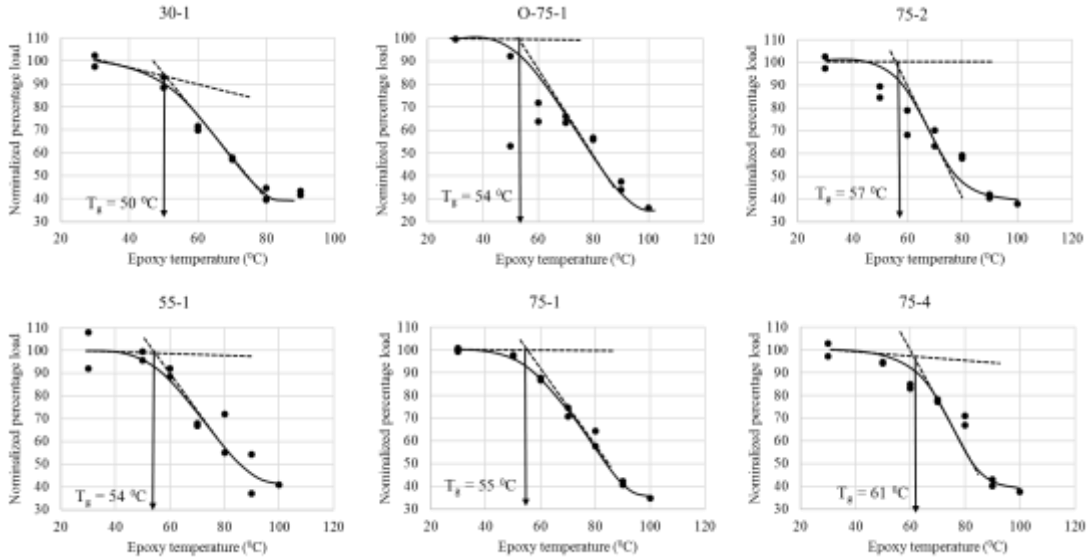

Figure 4.3Glass transition temperature for specimen groups

The figures indicate the evidence for increased bond properties with elevated temperature curing. Initial curing at elevated temperature for one hour has caused to 10% increase in T_g, irrespective of the exposed temperature level and the environmental condition, whether control or open nature. The period exposed to initial curing considerably affect on the bond performance. This clearly shows by the improved T_g from 10% to 20% with 1 hour to 4 hours of curing at the same temperature level. With high temperature curing the rigidity of the polymer chain of epoxy tends to increase (Wang et al. (2011)). This may happen with the four hours curing, while it partially occurs with the 1-hour curing at elevated temperature.

Gamage et. al. (2017) showed the increased resistance to long term environmental exposures to cyclic temperature, humidity and sustained loading with increased T_g. They further indicated the neutrality of bond for external environmental factors when the operating environment temperature is less than T_g + 20 ^{0}C of the bond. Hence, increased T_g of bond will enhance the service performance of the composite. Fire testing carried out by Ranasinghe et. al. (2011) showed the effectiveness and

economical application of an insulation layer for CFRP/concrete composites with increased T_g of the bond. Hence, it can be concluded that there is a possibility of increasing fire performances with increases T_g of the CFRP/steel bond.

4.1.4 Effects of Curing period at elevated temperature

The specimens shown in Figure.4.4 were exposed to the elevated temperature curing at 75 ^{0}C for 1, 2 and 4 hours. All these specimens cured at elevated temperature indicated higher strength than the ambient temperature cured specimens till the bond line temperature reaches 90 ^{0}C. This may due to the effect of high mobility of polymer chains at higher temperatures (Petrie (2006)) result in a more stable bond arrangement. Similar behaviour was noted from all the specimens tested by maintaining the bond line temperature more than 90 ^{0}C. This provides convincing evidence for degrading bond performance when the bond line temperature reaches 90 ^{0}C; i.e. 35^{0}C higher than the glass transition temperature of epoxy adhesive bond (T_g + 35^{0}C).

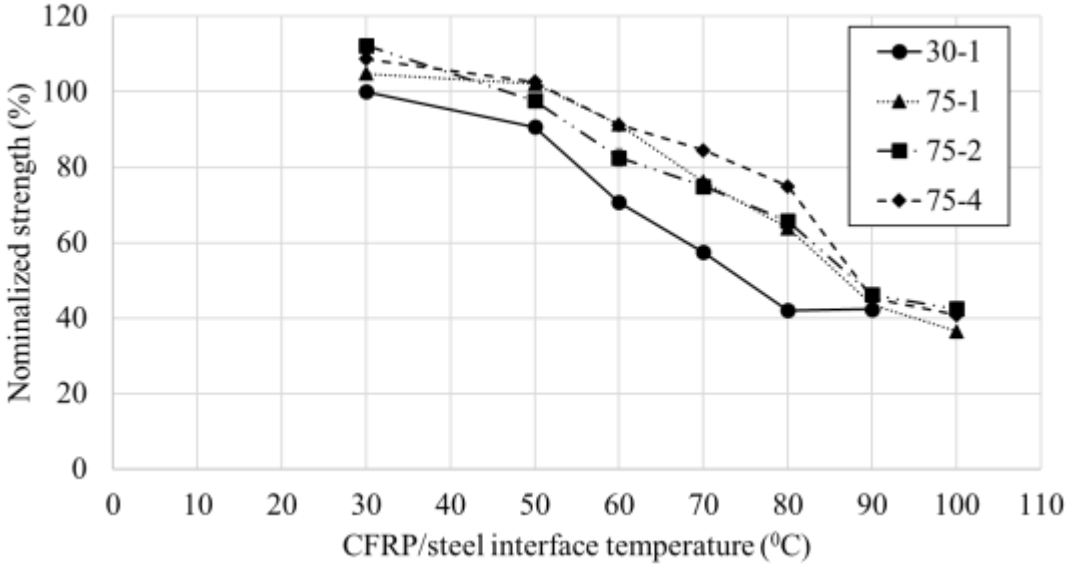

Figure 4.4 Effects of curing period on average failure load

4.1.5 Comparison between practical and experimental approaches for elevated temperature curing

In general, the majority of research work has been conducted in the controlled environments. In this study, curing the CFRP/steel composites in a standard oven to evaluate the effects of elevated temperature curing on bond characteristics is one of

an example. However, the nature of practical applications in civil engineering structures is completely different from the control environmental applications. Therefore, the comparison between these two approaches may help to understand the similarities or discrepancies in both cases.

Figure. 4.5 shows the joint capacities of ambient temperature cured and elevated temperature cured samples (at 75 ^{0}C for 1 hour) which were cured in the open environment using the halogen flood light system and in the control environmental chamber. Specimens from both techniques showed the similar trend in strength degradation. However, the samples cured in the practical approach indicated a slightly higher strength (17%) than the specimen cured under the control environment. This may due to the fact that elevated temperature allowed a ±5 ^{0}C margin when curing under open environment due to non-controllable nature. Due to this margin the temperature in the bond line could rise up to 80 ^{0}C while curing. Therefore, the use of research properties tested under the control environment can be taken as an indication of actual performance.

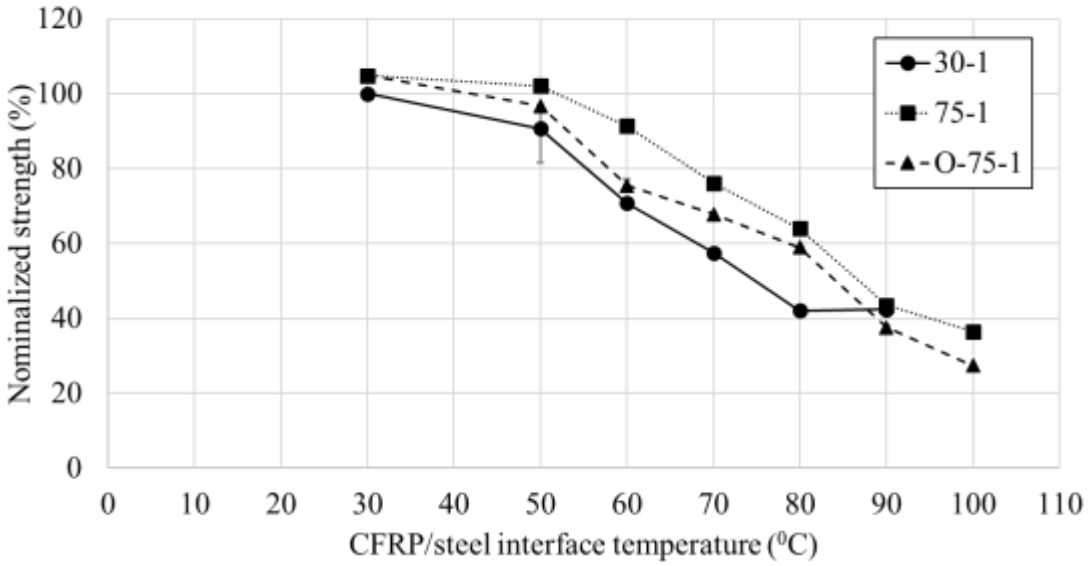

Figure 4.5 Comparison of elevated temperature curing using an oven and floodlight

4.1.6 Strain variation in CFRP sheet

Strain gauges were attached to the CFRP layer of double strap joints to measure the strain variation in both X and Y directions, 35 mm from the joint as described in

section 3. Strain measurement in X and Y directions when the bond line reaches the average temperature about 100 ^{0}C is shown in Figure. 4.6. Elastic region of the epoxy adhesive has increased with the curing temperature and curing time. The ultimate strain in CFRP of the elevated temperature cured samples has increased from 20% to 50%. However, all the tested samples had shown a plastic behaviour to rapid increase in the strain readings near failure.

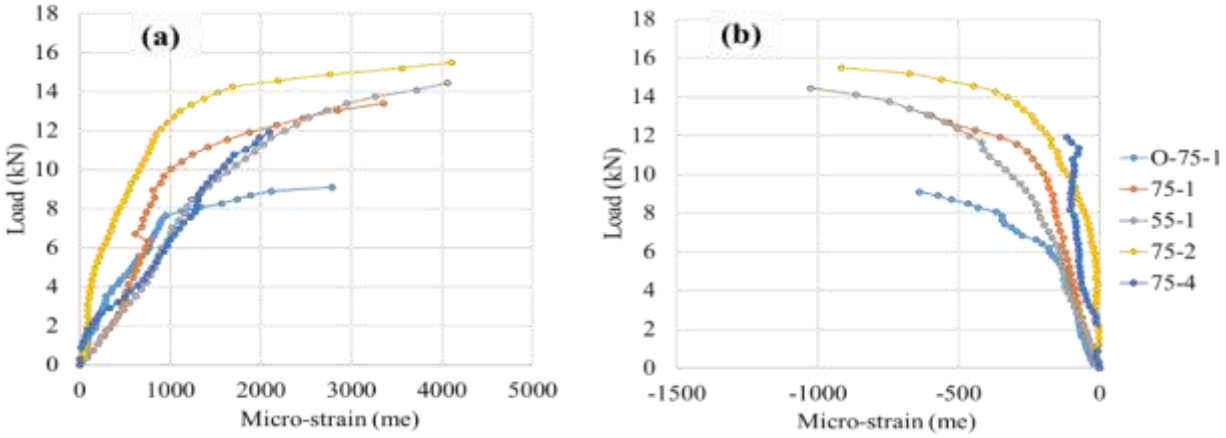

Figure 4.6 Strain variation on CFRP at 100 ^{0}C bond line temperature, (a) X (b) Y directions

4.1.7 Variation of Poisson's ratio

Figure. 4.7 shows the variation of poisson's ratio of the CFRP/epoxy/steel joint with the temperature in the CFRP /steel interface. At a low temperature level which is below 60 ^{0}C, the Poisson's ratio has a significant change with the curing temperature and curing time of the specimen. The Poisson's ratio had increased with the curing temperature and the curing period. When the curing temperature increases from 55 ^{0}C to 75 ^{0}C, the Poisson's ratio increases up to 4%. One-hour increase of curing time had caused for 7 % increment in the Poisson's ratio. When the temperature is more than 70 ^{0}C [$\geq$ (T_g + 15 ^{0}C)] all the specimens indicated a high rate of reduction of the Poisson's ratio in the similar manner.

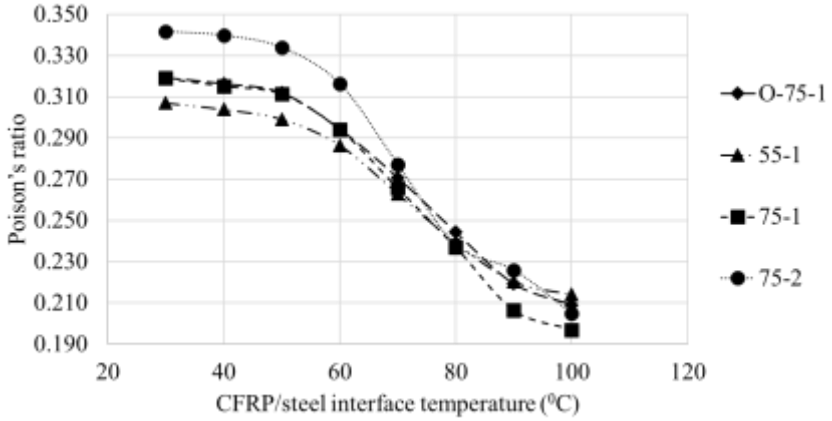

Figure 4.7 Variation of Poisson's ratio with bond line temperature

4.1.8 Variation of Elastic modulus

The variation of Elastic modulus of the bond with the bond line temperature is shown in Figure. 4.8. Elevated temperature curing has a significant effect on the elastic modulus up to the bond line reaches 80 ^{0}C. On average, 50% increase in elastic modulus has found from the composites cured at 75 ^{0}C for four hours. However, the variance of elastic modulus has grown thin when the bond line temperature reaches 80 ^{0}C. The effect of curing temperature and curing time had not considerably affect on the elastic modulus of the bond when the interface temperature exceeds 80 ^{0}C.

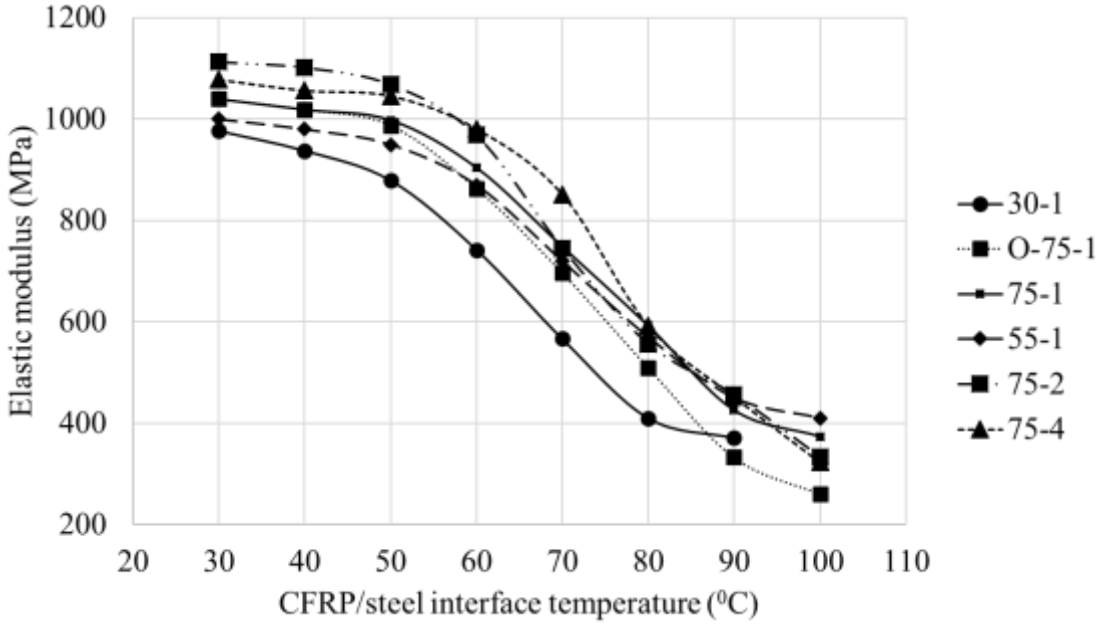

Figure 4.8 Variation of Elastic modulus with bond line temperature

5. THEORY OF FE ANALYSIS AND PRELIMINARY MODELING

Numerical investigation helps to mitigate the time consumption and cost involved in experimental investigations. Numerical analysis also helps to contract a time consuming, complex experimental procedure into a computer program which will present a wide range of results as in an experimental investigation without consuming huge time and cost. Finite Element Analysis (FEA) or Finite Element Method (FEM) is a popular mode of numerical analysis method which is being used worldwide, which will generate results required in a civil engineering investigations such as deflection, stresses, strains, loads, reactions etc. Main principles which are used in FEA in a structural mechanics are energy principles such as the virtual work principle or the minimum total potential energy principle.

A three dimensional model was developed to predict the bond characteristics between CFRP and steel plate. Effect of different surface preparation techniques and elevated temperature curing was modelled by varying the properties of interfaces. This chapter presents the background of theoretical model procedure, analysis, validation and parametric studies.

5.1 Finite Element Analysis

Most of the time Finite Element Analysis theories are very complex to use with manual calculation in large models. Therefore, the computer softwares were created by using the Finite Element Analysis theories to apply them in the real life complex models. The applicability of a such software can be changed based on its constitutes, such as the theories which used in a computer program, the input data which is required by the program and the output results which will be shown at the termination of the programme.

ANSYS is an engineering simulation and 3-D design software which has a wide range of applicability from basic structural engineering to electromagnetic engineering applications. ANSYS 14 is a modern version of a series of FEA software

which was developed by ANSYS, Inc., an American software company (ANSYS mechanical user's guide, 2013).

The main finite element theory which is used to analyze a structural system consist the following main steps,

1. Discretization of the structure and selection for proper interpolation model. Define unknown degrees of freedom at each node and the actions to be determined for any element.
2. Under the loading determine restraining forces to prevent displacements. Also determine values of actions for any element with nodal displacement prevented.
3. Generate the structure stiffness matrix by an assemblage of element displacements. Also generate actions due to unit displacements at coordinates.
4. Formulate the equilibrium equations to meet the general theories of structural mechanics and physics.
5. Calculate the required stress components for each element with solving the equilibrium equations.

However, when the finite element analysis is done using a computer, the most of the above steps would be executed by the computer software itself. However, it is required to enter the proper conditions to simulate the situation by the user of the software. Otherwise, the simulation can vary from the actual one or the simulation itself can be completely different from the actual scenario.

The procedure of finite element analysis programme can be divided into three main parts.

- Pre-processing
- Processing (solving)
- Post-processing

Pre-processing includes the defining geometry of the structure, defining material characteristics and dividing the structure into elements. When defining the geometry, it is not necessary to generate the entire actual structure in the finite element model. However, the finite element model should represent the accurate mathematical model of the actual structure. In material properties, it is important to define the material properties which are needed to have the possible outcome. In other words, the definition of the material characteristics is based on the output results which are desired at the end of the simulation. Other main step in pre-processing is defining the mesh. Meshing is a process which involves selecting the element types (quad, triangular, brick, shell etc.), element sizes, aspect ratios. The above factors have to be defined according to the geometry, material models and the accuracy required at the end of the solving.

Processing or solving will be executed by the computer itself, which the user can only control it by providing the solver times, steps and other basic requirements only. The finite element theory which was discussed in an above paragraph will be used in this process by using the data input in the preprocessing step. However, this process may display errors or warnings due to the bugs and errors which were happening in pre-processing step. However, in this process a termination can happen due to the size of the simulation which would be a result of high mesh density.

Post-processing is the step which will generate the results required in the investigation. This process may include the transformation and extrapolation of the results which were generated in the solving process. Those transformed and interpolated results may be visualized in a manner that can be observed and compared according to the user's preferences.

5.2 Finite Element Model

5.2.1 Geometry of the model

In the test series specimen size was selected as in listed in Table 3.1,

Table 5.1 Actual specimen dimensions

	Length	Width	Thickness
Steel plate (single side)	160mm	40mm	3.8mm
Adhesive layer (two layers)	Vary	40mm	0.451mm
CFRP layer (two layers)	Vary	40mm	0.166mm

The thickness of the steel plates and CFRP layers were measured and thickness of the adhesive layer was calculated using the following Eqs (3.1).

$$t_a = (t-t_s)/2 - t_{cfrp} \quad \ldots\ldots(3.1)$$

t_a = thickness of adhesive layer

t = total thickness of the specimen

t_s = thickness of steel plate

t_{cfrp} = thickness of CFRP layer

5.2.2 Effective bond length

In the experimental series different bond lengths were varied to find the effective bond length for CFRP steel double strap joints for the tested materials. A range of bond lengths were described in the test programme as described in section 3. The models with the same dimensions were developed. An axi-symmetric model was developed (Figure 5.1) for simulations to reduce the time consumption for analysis. Hence, one eighth of the actual specimen was modelled in the finite element analysis.

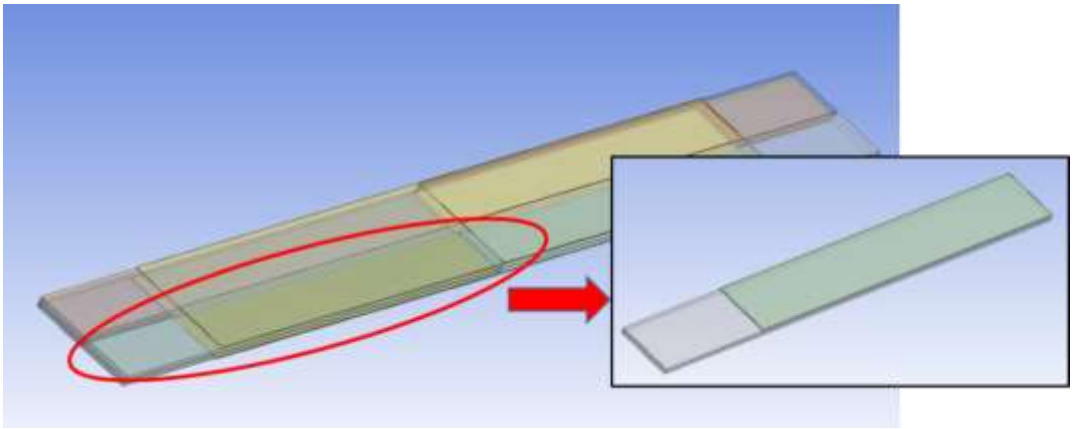

Figure 5.1 ***Actual specimen can be divided into eight equal parts considering symmetry***

5.2.3 Material Models

Steel properties were acquired from a steel coupon test which was done according to the ASTM A 370-02 (Standard test methods and definitions for mechanical testing of steel products). It was modeled as a non-linear material. The direct stresses were considered as material coupon was failed in the middle of the coupon.

Table 5.2 ***Measured mechanical properties of steel***

Property	Tensile strength (MPa)	Ultimate strain	Elastic Modulus (GPa)	Poison's ratio
Value	583	0.065	200	0.3

Adhesive (Araldite 420) properties were acquired from an adhesive coupon test done according to the ASTM D638-02(a) (Standard test method for tensile properties of plastics) standards. The material was modeled as a Bilinear material in ANSYS (ANSYS mechanical user's guide, 2013). Direct stresses were considered as the material was failed in the middle of the coupon.

Table 5.3 ***Measured mechanical properties of adhesive***

Property	Tensile strength (MPa)	Ultimate strain	Elastic Modulus (GPa)	Poison's ratio
Value	29	0.046	0.977	0.3

CFRP layer properties were acquired by a CFRP sheet test done according to the ASTM D3034/D3039M (Standard test method for tensile properties of polymer matrix composite materials) standards. CFRP layer properties were also given as a bilinear material model. As the CFRP layer was failed in the middle of the specimen in the experiments the direct stresses were considered in modelling.

Table 5.4 ***Measured mechanical properties of CFRP***

Property	Tensile strength (MPa)	Ultimate strain	Elastic Modulus (GPa)	Poison's ratio
Value	1575	0.009	175	0.3

5.2.4 Boundary conditions

The symmetry of the specimen was considered in the modeling. Therefore, proper constraints have to be assigned on the faces, where the symmetry of the model is identified as shown in Face B, C and D. There are three faces where the symmetry of the specimen is considered. Displacements were not allowed on X, Y and Z directions respectively on the faces B, C and D. Rotations were all restricted on all the directions on symmetrical planes. The load was applied on the steel plate opposite to the joint as a transient displacement with the load steps of 50 till the failure.

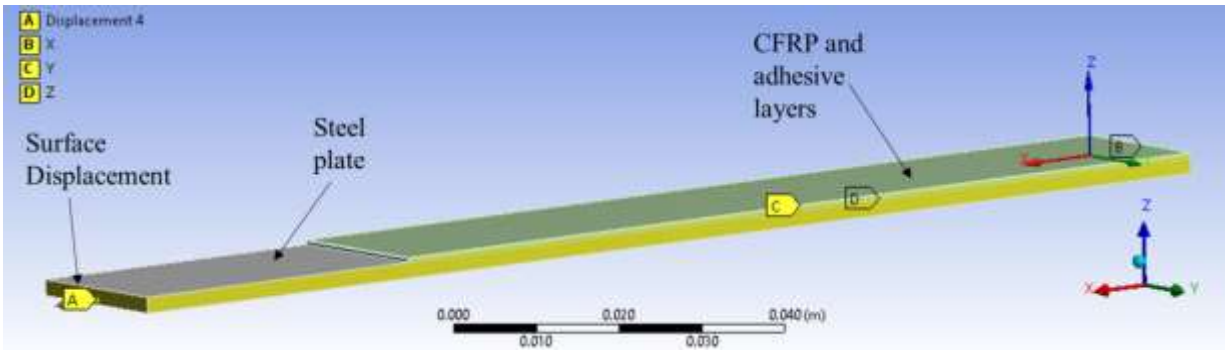

Figure 5.2 ***Boundary conditions and loads on FE model***

5.2.5 Mesh and solver

The meshing of the structure is the main step that defining the constitute of the model and defining the constitute equations in the elements. In this step it would define the element types which will be going to use in the analysis. As the double strap joint is consisted with three different types of materials, those were modelled as plate elements. SOLID 185 elements type which (Figure 5.3) defined with 8 nodes were used to model the steel plate while SOLID 186 elements (20 nodes) were used to

model the adhesive layer. SHELL 281 elements with 8 nodes were used to model the CFRP sheet.

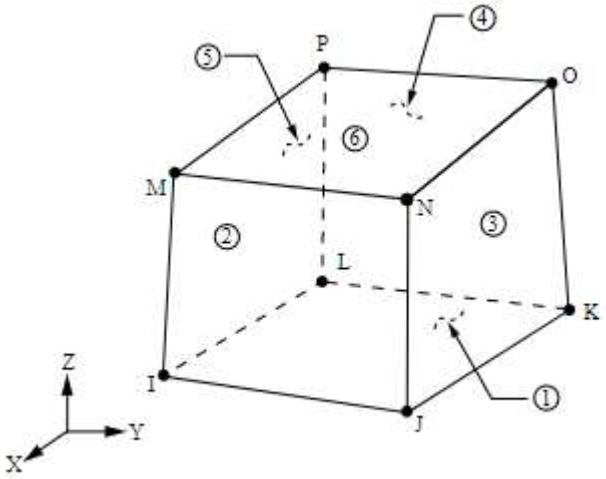

Figure 5.3 SOLID 185 element

SOLID 185 (Figure 5.4) elements were used for modelling the 3-D solid structures. The element consisted with eight nodes having three degrees of freedom at each node, translations in nodal x, y and z directions. SOLID 185 capable to calculate plasticity, hyperelasticity, stress stiffening, creeps, large deflection, and large strain. Therefore, it is more than capable of defining the larger strains in the steel plates due to the non-linear analysis.

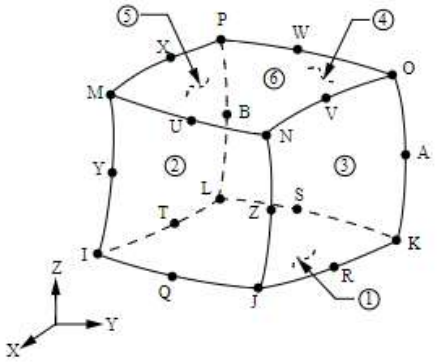

Figure 5.4 SOLID 186 element

SOLID 186 elements (Figure 5.5) are a higher order 20 node element which exhibits the quadratic displacement behavior. SOLID 186 element capable of calculating plasticity, hyperelasticity, creep, stress stiffening, large deflection, and large strain same as the SOLID 185 element. This element also has three degrees of freedom in

each node, translations in nodal x, y and z directions. As this is higher order finite element type, it is more suitable for adhesive layer which will present to perform more accurate results compare to SOLID 185 element. However, much more analysis time will be required in the analysis as the constitute of the element is more complex.

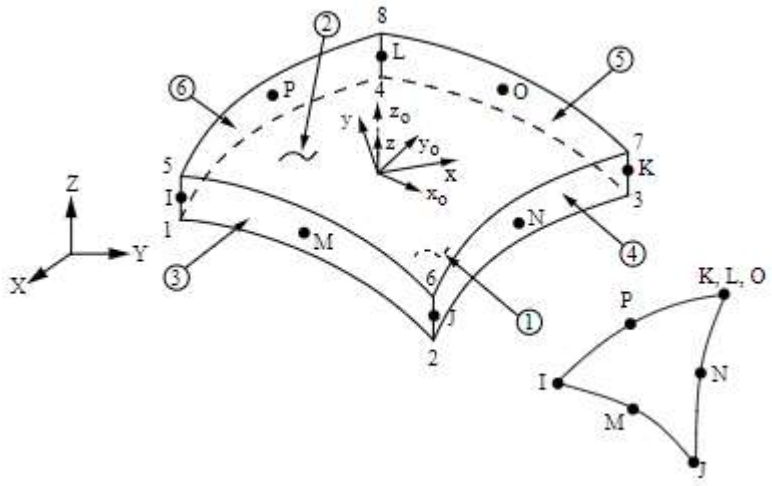

Figure 5.5 SHELL 281 element

SHELL 281 is an element with eight nodes and six degrees' freedom in each element, translation around x, y and z axes, rotation around x, y and z axes. These elements are used in linear, large rotation, and/or large strain nonlinear models. This SHELL 281 element is more suitable for modeling composite shells or sandwich construction, which is the case in the steel CFRP double strap joints.

Mesh sensitivity of the structure plays an important aspect on the accuracy of the outcome of the analysis. However, the mesh sensitivity can effect on the analysis size and analysis time. Therefore, it is important to choose the effective mesh sensitivity according to the resources available and accuracy required at the end of the analysis.

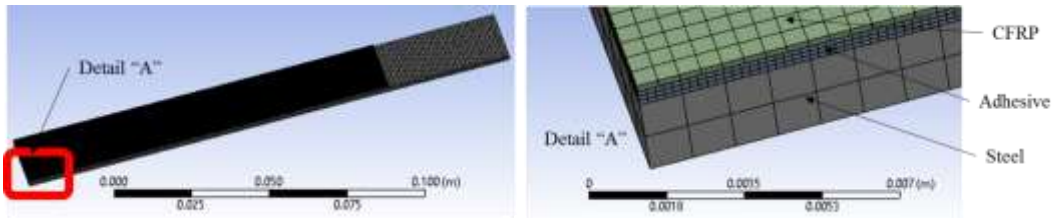

Figure 5.6 *Finite Element Mesh*

Therefore, using of effective mesh is necessary to gain accurate results and reduce the processing time. However, then it is not effective to use same mesh sensitivity over the entire model. Therefore, the mesh sensitivity was determined based on the critical areas of the model which were required high accuracy. The adhesive layer is a part where high accuracy is required in modelling. Therefore, it was meshed to have 0.1 mm mesh size for adhesive layer, while the 1 mm mesh was used for steel plate. The mesh size of the CFRP was chosen to be 0.166 mm which is the thickness of the CFRP sheet (Figure 5.6). The aspect ratio was used as 1:1 for all elements, which were eventually became square elements. Processor of 8 GB RAM was used along an i7 intel processor to solve the model. Time between 2-4 hours was consumed to complete the analysis.

5.3 Predicted Effective bond length for CFRP/steel double strap joints

Ultimate bond strength was observed for different bond lengths in experimental series and FE modelling. Initially, the same aspect was modelled in the ANSYS finite element analysis software. The bond lengths of 40 mm, 75 mm, 90 mm, 100 mm, 110 mm and 120 mm were modelled and the results were compared with the experimental results. The average discrepancy between tested and predicted results was 15 % indicates the accuracy of the model as shown in Fig 5.7. Then the parametric study was conducted to evaluate the bond strength with the CFRP bond lengths which were not tested.

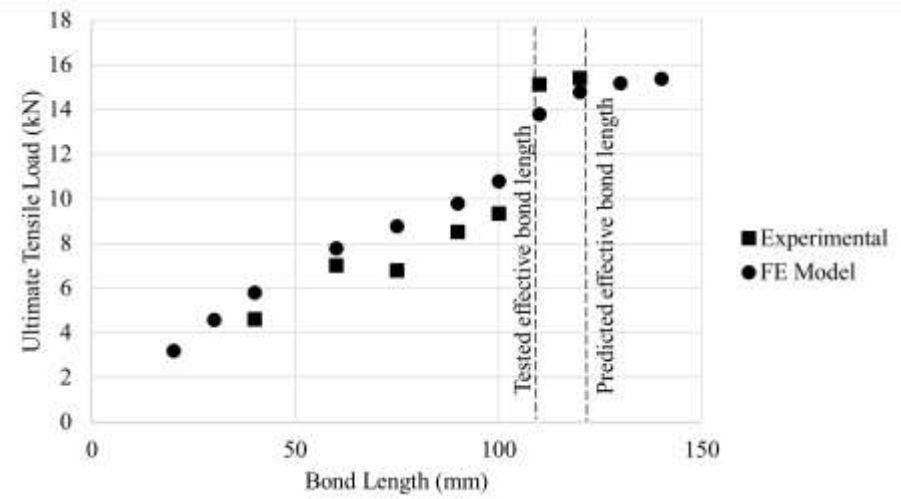

Figure 5.7 ***Comparison between predicted and tested bond lengths***

According to the Figure 5.7 the model predicted ultimate load deviate on average 15% from the experimental results. Experimentally determined effective bond length is 110 mm. However, the model predicted effective bond length varies between 110 mm and 120 mm differs up to 10 mm from the experimental results. The selected bond length 110 mm for further investigations is in good agreement with the tested and predicted ultimate strength values.

6. NUMERICAL MODELLING AND BOND SHEAR STRESS SLIP BEHAVIOR OF CFRP/STEEL JOINTS CURED AND TESTED AT ELEVATED TEMPERATURE

6.1 Material Properties

Measured material properties at ambient temperature (30 ^{0}C) were used in modelling as listed in Table 6.1.

Table 6.1 Material properties at ambient temperature

Material Property	Steel	Adhesive	CFRP
Average Tensile strength (MPa)	583	25	1575
Average Ultimate strain	0.065	0.043	0.009
Average Elastic Modulus (GPa)	200	0.579	175.62
Average Poison's ratio	0.3	0.3	0.3

The bond behavior at elevated temperature was studied during the test programme. Since, the adhesive component is critical and sensitive to the temperature, degradation of material properties of adhesive bond with the temperature were considered [Figure. 6.1]. It was assumed that the variation of material properties of steel and CFRP are negligible compared to the mechanical properties degradation of adhesive bond within the considered temperature range for modelling.

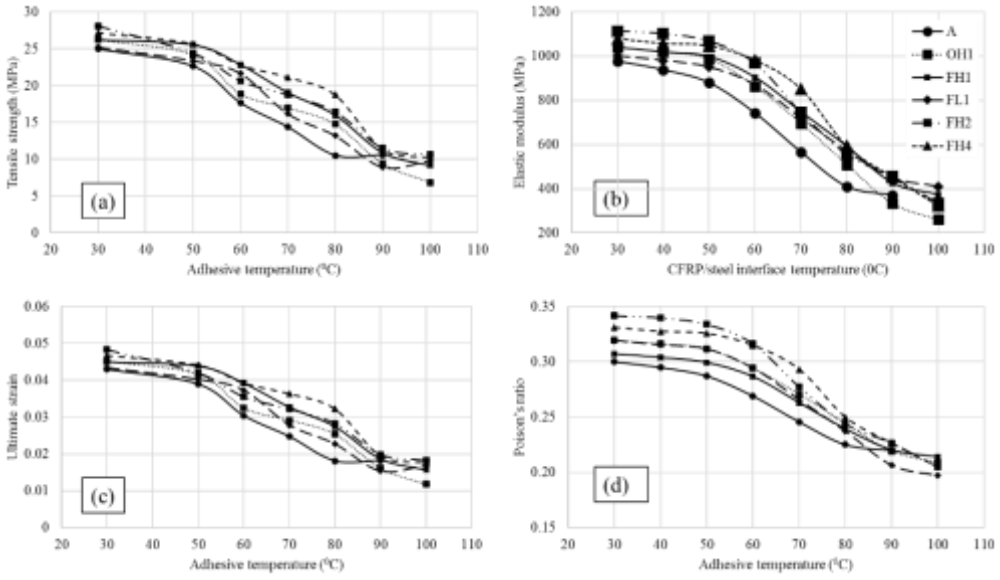

Figure 6.1 Variation of adhesive properties with temperature (a) Tensile strength (b) Elastic modulus (c) Ultimate strain (d) Poison's ratio

6.2 Transient heat analysis

Transient heat analysis was performed using transient thermal tools in the software (ANSYS mechanical user's guide). The thermal behavior of the CFRP/steel double strap joints were predicted for the variation of environmental temperatures (t_e) with time. Figure. 6.2 (a) shows the variation of bond line temperature for different environmental temperatures. It has shown that the bond line temperature reached the environmental temperature within 5 minutes of exposure to the temperature changes. Figure. 6.2 (b) indicates the uniformity of the temperature distribution within the bond line after saturation within a short period (<5 minutes). This is clearly indicating the non-insulation properties of CFRP as observed in CFRP/concrete composites (Gamage et al, 2006). Thermal expansion effects of materials used in CFRP/steel double strap joints were considered negligible at temperature levels less than 100 ^{0}C.

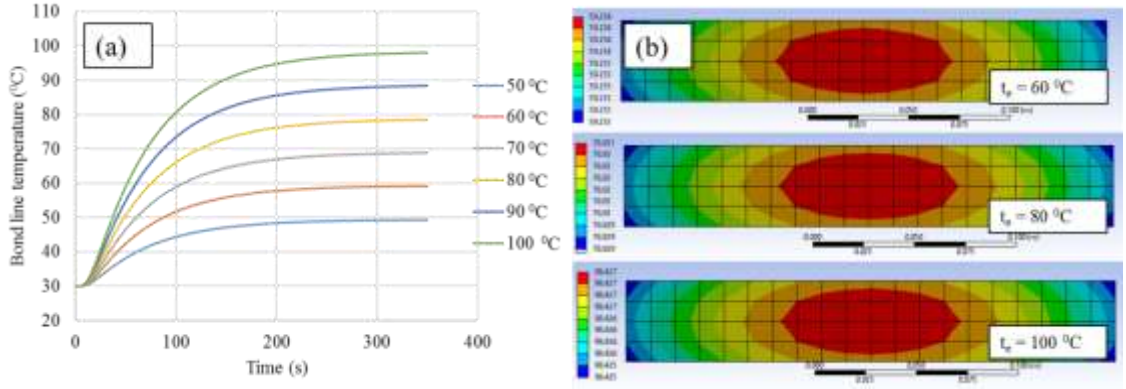

Figure 6.2 (a) Bond line temperatures of CFRP/steel joints for different t_e (b) Temperature contours of bond for different t_e

6.3 Thermo-mechanical analysis

Thermo-mechanical analysis was performed at low temperature range to identify the detailed bond mechanism which cannot be measured during testing for non-insulated CFRP/steel composites. ANSYS Mechanical APDL was used as the solver in thermos-mechanical analysis. The load boundary conditions were applied as described in section 3.1. Initially the transient heat analysis was performed. Then the temperature variation within the bond line was used to arrange the property

degradation with the temperature. Finally, a transient load was applied to the joint till failure.

6.4 Model results and validation

Comparison between the average experimental joint capacities (P_{EXP}) and predicted load capacity (P_{FE}) results are shown in Figure. 6.3. It was observed that P_{FE}/ P_{EXP} ratios are in the range from 1.005 to 1.104 for all the models. Predicted results for each conditions have shown a slight higher values than the average experimental failure load in each scenarios. The deviation between predicted and experimented failure loads lie in the range between 4% and 10%, when the exposed temperature increases from 30 ^{0}C to 100 ^{0}C. The average coefficient of correlation is 1.087. This clearly indicates the accuracy of model for predicting the joint capacity. The temperature exposure beyond 100 ^{0}C were not considered for the analysis since the retained strength of joint at this temperature is less than 20%.

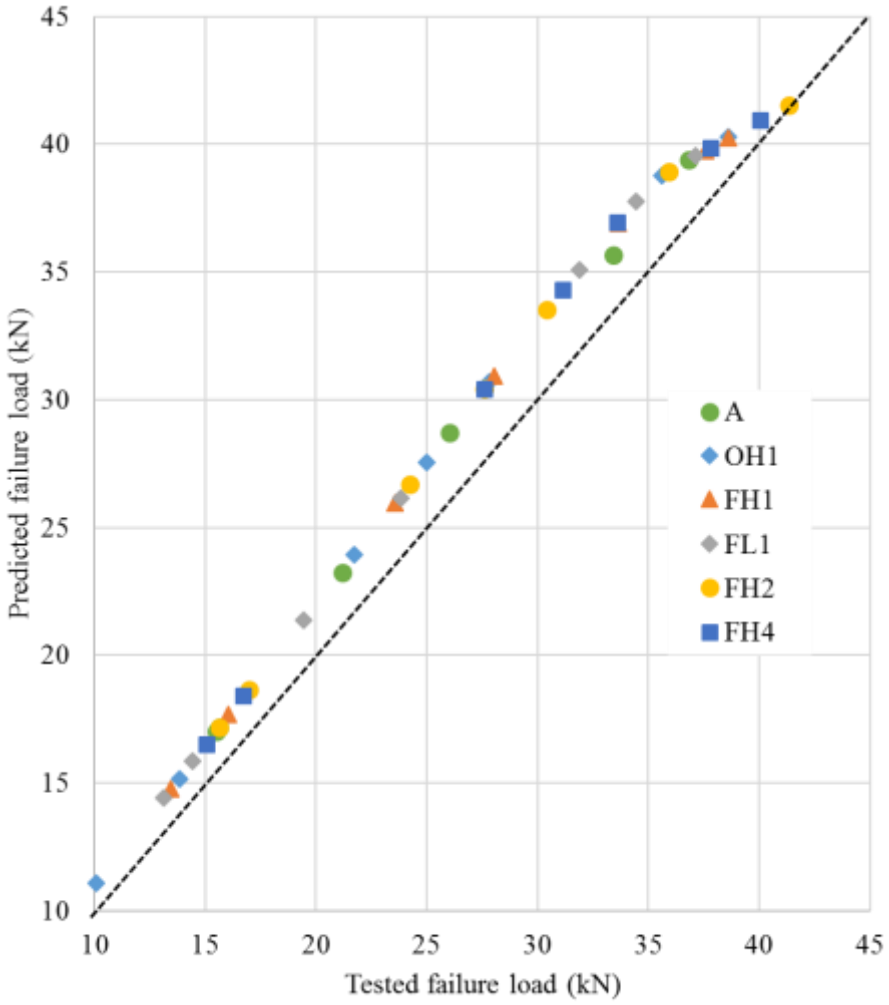

Figure 6.3 Correlation between experimental and FEM failure loads

Measured and predicted strain variations in both X and Y directions at 35 mm from the joint, which exposed to 100 ^{0}C environmental temperature are shown in Figure. 6.4. Both predicted and experimental data have shown an elastic behavior at the beginning of the loading. The discrepancy in predicted and experimented values within this region are less than 10%. However, the start of the plastic behavior has begun at about 6 kN load level in the developed numerical model to simulate the bond characteristics, while experimental data have shown the start of plastic behavior at about 8 kN load level. Predicted strain values in the CFRP with in the plastic range shows on average 12% difference compared to the experimental results. Hence, the accuracy in strain behavior can also be expected.

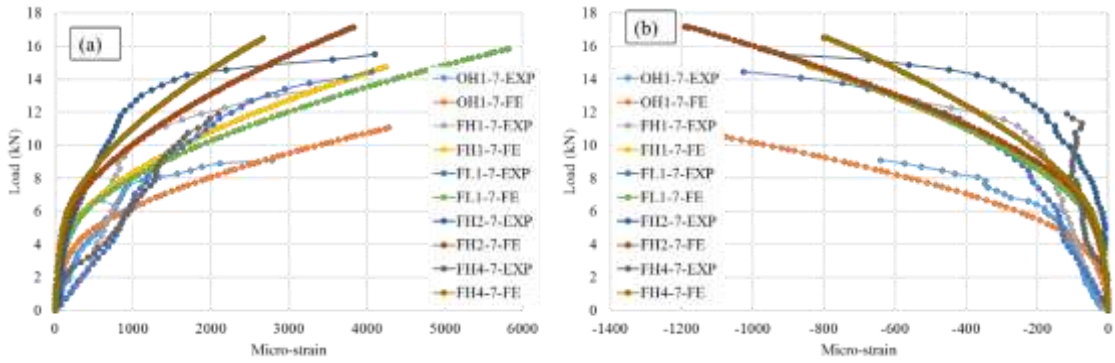

Figure 6.4 Strain variation on CFRP at 100 ^{0}C bond line temperature for experimental and FEM results, (a) X (b) Y directions

The stress variation contours of the CFRP sheet and within the adhesive bond line near failure are shown in Figure. 6.5 at different bond line temperatures for the ambient temperature cured samples. The most common failure mode observed when the bond line temperature is less than 60 ^{0}C is the combination of CFRP rupture and the interface debonding. The predicted stress contours of samples tested below 60 ^{0}C also indicated the similar nature as shown in Figure. 6.5. In the test programme, the interface debonding failure was often observed for the samples tested above 60 ^{0}C. The predicted stress variations have also shown high stress concentrations in the adhesive layer when the bond line temperature exceeds 60 ^{0}C.

Bond line temperature (^{0}C)	CFRP layer stress (MPa)	Adhesive layer stress (MPa)	Predicted stress (MPa)		Remarks
			CFRP	Adhesive	
30			1575	25	Both CFRP and adhesive stresses have reached their ultimate values. Combined failure in CFRP and adhesive layers.
50			1552	22.6	Both CFRP and adhesive stresses have reached their ultimate values. Combined failure in CFRP and adhesive layers.
60			1459	17.6	Only adhesive layer stress has reached its ultimate value. Failure in adhesive layer.
70			1364	14.3	Only adhesive layer stress has reached its ultimate value. Failure in adhesive layer.
80			1231	10.5	Only adhesive layer stress has reached its ultimate value. Failure in adhesive layer.
90			1235	10.6	Only adhesive layer stress has reached its ultimate value. Failure in adhesive layer.

Figure 6.5 Stress contours at near failure

6.5 Bond shear stress vs slip

6.5.1 Effects of bond line temperature

Temperature has influenced significantly on the bond slip relationship for all six specimen groups exposed to elevated temperature curing at different temperature levels as shown in Figure. 6.6. All the samples had indicated an average 0.17 mm initial slip, 0.43 mm maximum slip and 26 MPa maximum shear stress at 30 ^{0}C bond line temperature. When the bond line exposed to the temperature of 90 ^{0}C, the respective values (initial slip, maximum slip and maximum shear stress) have changed to 0.15 mm, 0.35 mm and 9 MPa. Therefore, when the bond line temperature increases from 30 ^{0}C to 100 ^{0}C, on average 17%, 60% and 25% reductions of initial slip, maximum shear stress and maximum slip, respectively were noted, irrespective from the curing condition. These reductions are negligible till the bond line reaches 50 ^{0}C for ambient temperature cured samples. The latter for elevated temperature cured samples is 60 ^{0}C. This clearly indicates the weaken bond properties with the exposure to the elevated temperature, which indicates the importance of providing an insulation layer for CFRP/steel composites cured under any condition.

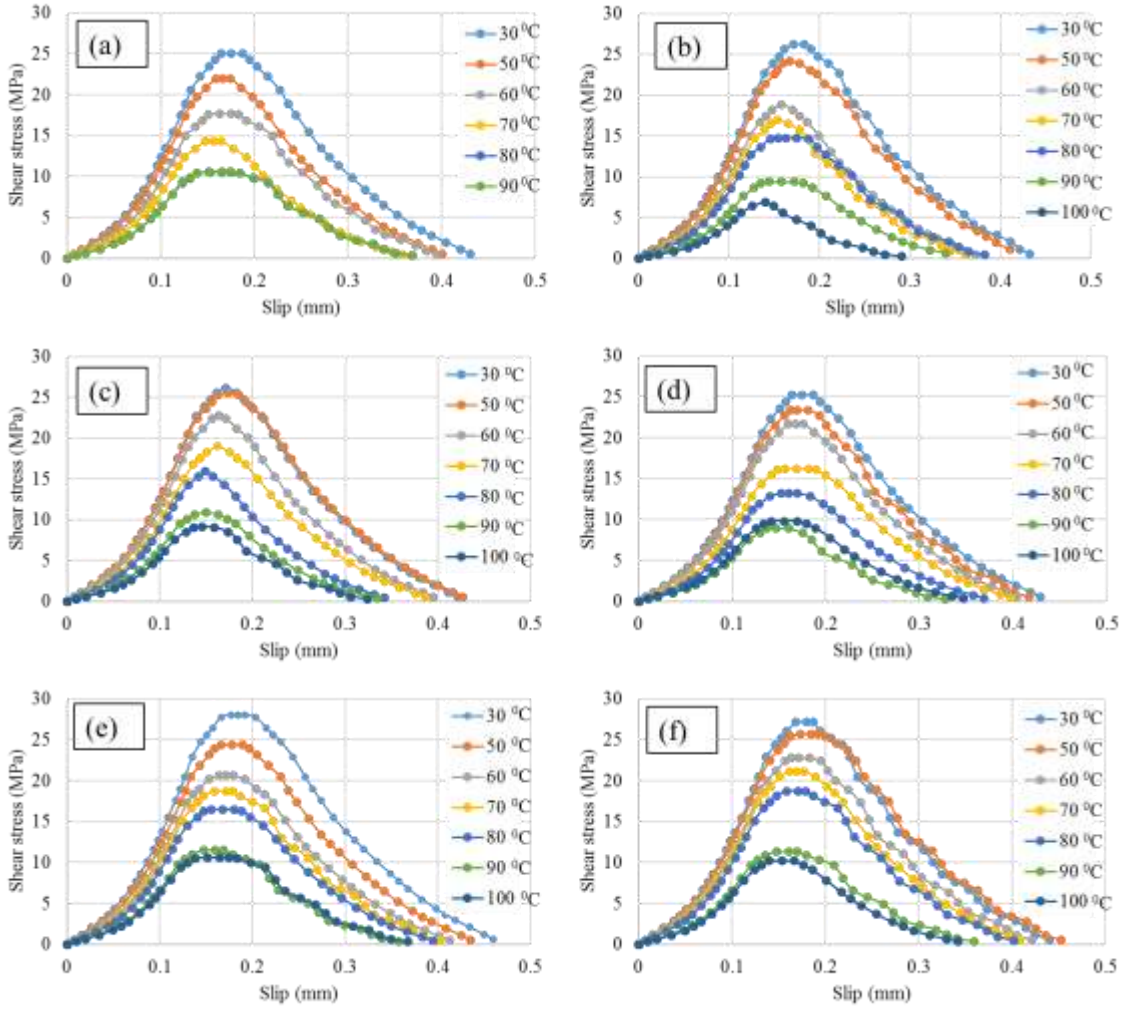

Figure 6.6 Effect of bond line temperature on bond slip vs shear stress for different curing conditions for specimen groups, (a) A (b) OH1 (c) FH1 (d) FL1 (e) FH2 (f) FH4

6.5.2 Effects of curing condition

The behavior of CFRP/steel composites at different temperature levels with respect to their curing conditions is shown in Figure. 6.7. The curing condition has shown a minimum effect at the low bond line temperatures (<50 ^{0}C), while the maximum effects at the high bond line temperatures (80 ^{0}C, 90 ^{0}C and 100 ^{0}C). When the system exposed to ambient conditions (30 ^{0}C), the change in initial slip, maximum slip and maximum shear stress were 5%, 9% and 10%, respectively. When the bond line reaches the temperature higher than 70 ^{0}C, initial curing condition of the system starts to influence significantly on the bond line properties as shown in Figure. 6.7 (a) to 6.7 (g). However, at 100 ^{0}C the bond line temperature, initial and maximum slips and maximum shear stress values have decreased by 12%, 17% and 47%,

respectively with the type of curing. Figure. 6.7 (g) indicates a considerable effects of curing condition on bond line properties at relatively high temperature levels. This clearly indicate the importance of initial curing condition on the performance of CFRP/steel composites exposed to elevated temperature.

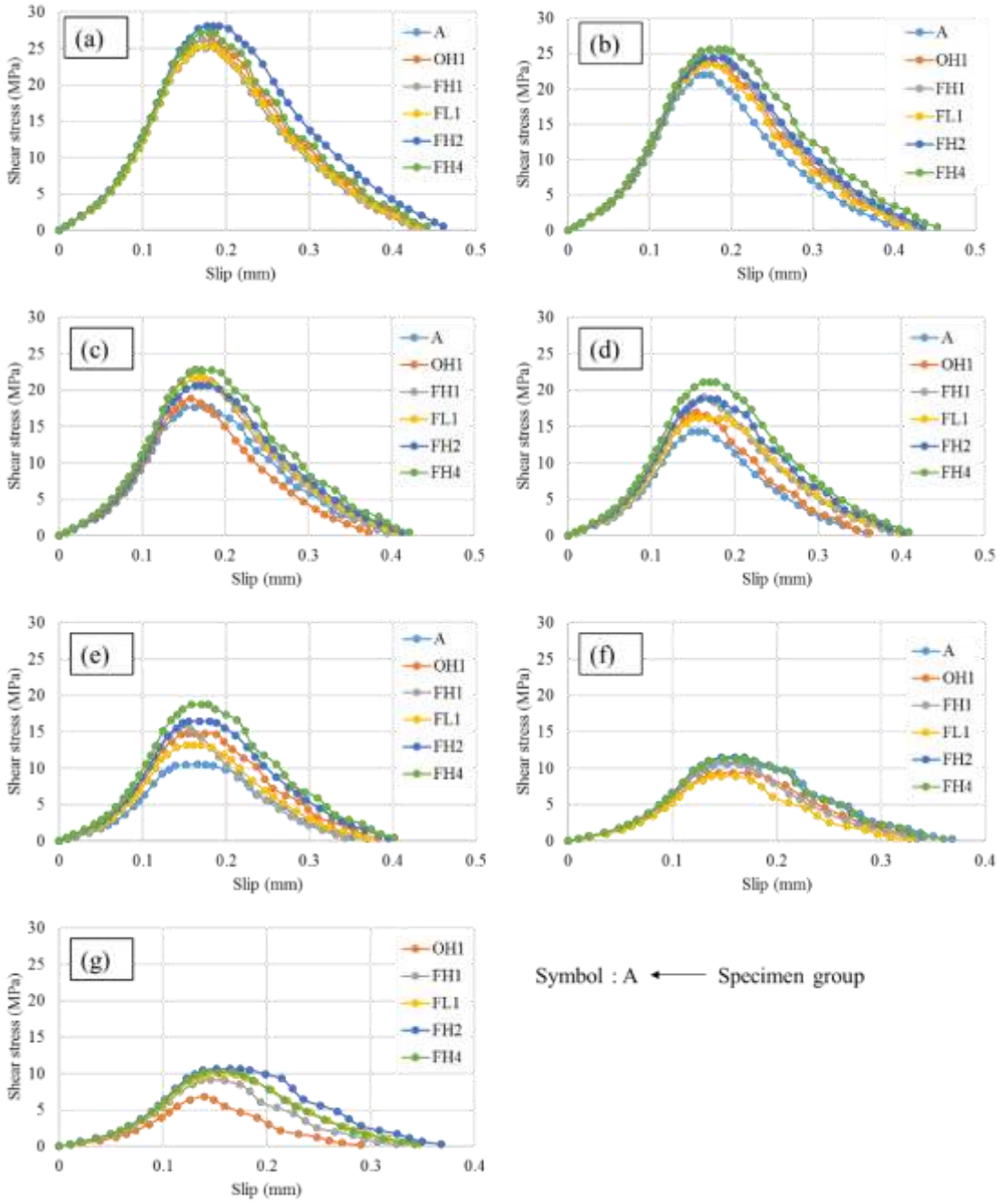

Figure 6.7 Effect of curing condition on bond slip vs shear stress for bond line temperatures, (a) 30 ^{0}C (b) 50 ^{0}C (c) 60 ^{0}C (d) 70 ^{0}C (e) 80 ^{0}C (f) 90 ^{0}C (g) 100 ^{0}C

6.6 Parametric study

6.6.1 Effects of adhesive layer thickness

Effects of adhesive layer thickness of the ambient temperature cured samples (A) and the samples with initial 75 ^{0}C temperature curing for 4 hours are shown in Figure. 6.8. Adhesive layer thicknesses at bond line; 0.5 mm, 1.0 mm, 1.5 mm and 2.0 mm were chosen for the study. On average 200% and 130% increase of initial slip and maximum slip, respectively has observed when the adhesive thickness increases from 0.5 mm to 2.0 mm for both curing conditions at considered temperature exposure range. However, the maximum shear stress of the joint has not been affected by the thickness of adhesive layer. The area enclosed by the bond shear stress-slip curve has increased with the elevated temperature curing. This means the fracture energy of bond has increased when the system cured under elevated temperature result in more stable bond.

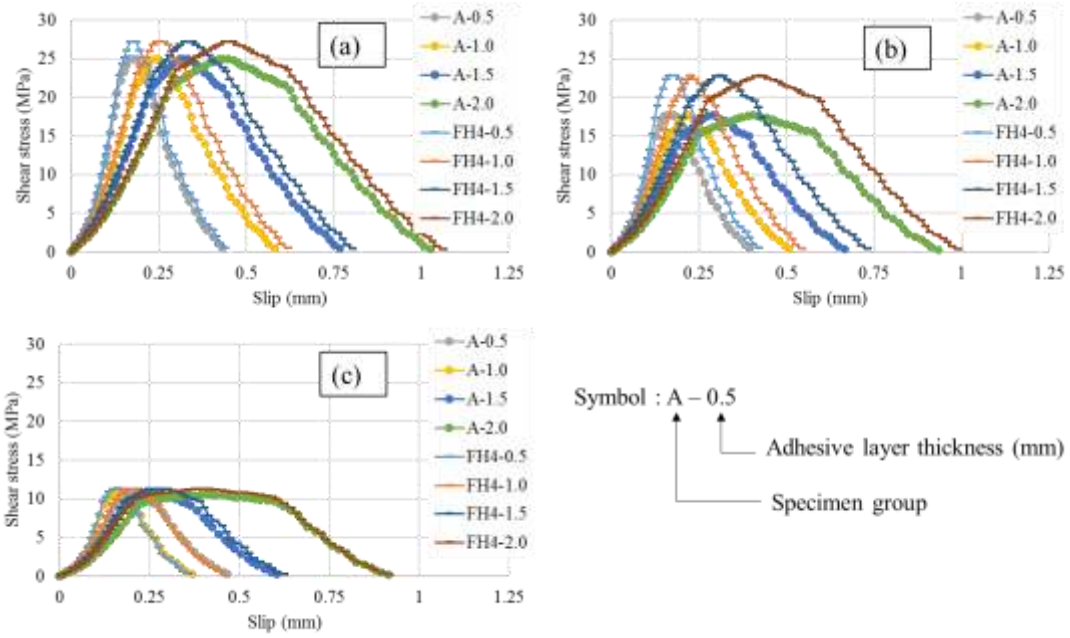

Figure 6.8 Effects of adhesive layer thickness on bond slip vs shear stress for bond line temperatures, (a) 30 ^{0}C (b) 60 ^{0}C (c) 90 ^{0}C

6.6.2 Effects of CFRP layer type

An another important aspect is to evaluate the bond properties at elevated temperature with respect to the curing condition and type of CFRP material used for

strengthening. Three types of CFRP fabrics were chosen including the one used in the experiment (General purpose). The mechanical properties of other two types (High modulus and Ultra high modulus) used in modelling are listed in Table 6.2.

Table 6.2 CFRP fabric properties

CFRP type	Elastic modulus (GPa)	Ultimate strength (MPa)	Ultimate strain
High Modulus (HM)	330	2500	0.005
Ultra-high modulus (UHM)	600	2000	0.002
General purpose (GP)	175	1575	0.009

Effects of CFRP fabric types on bond slip relationship are shown in Figure. 6.9 for bond line temperatures, 30 ^{0}C, 60 ^{0}C and 90 ^{0}C. A significant difference cannot be observed in the initial slip and maximum shear stress for different CFRP fabric types. The maximum shear stress in the bond slip relationship varies only with curing method. However, UHM CFRP fabrics have shown 4% less maximum slip compared to the GP and HM CFRP types at all level of temperature exposure. The curing condition has also significantly affected on the bond slip model only beyond the temperature exposure of 60 ^{0}C.

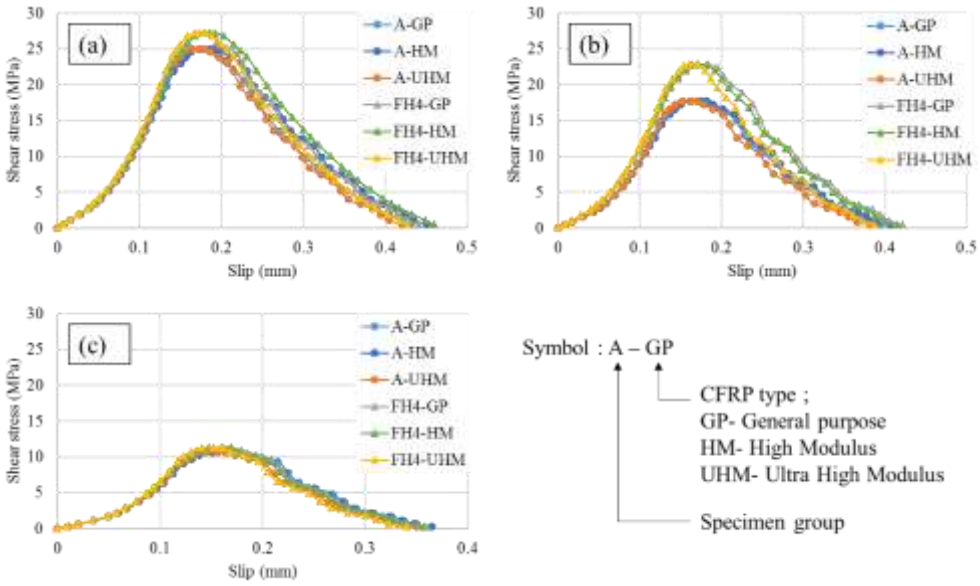

Figure 6.9 Effects of CFRP type on bond slip vs shear stress for bond line temperatures, (a) 30 ^{0}C (b) 60 ^{0}C (c) 90 ^{0}C

6.6.3 Effects of CFRP layer thickness

To check the effect of CFRP layer thickness on bond slip relationship, three commercially available CFRP thicknesses for general purpose CFRP were used (X-Wrap C230, X-Wrap C530) as shown in Figure. 6.10. CFRP layer thickness had also shown a minimum effect on the initial slip and the maximum shear stress for all considered bond line temperature exposures and the curing method. The thickness of selected CFRP sheet does not affect on the bond shear stress- slip behavior as shown in Figure. 6.10. This may due to low effects of temperature on CFRP material compared to epoxy adhesive (ARELDITE 420 A/B, X-Wrap C300). The curing method had influenced only on the maximum shear stress of the composite. However, on average 7% difference has been observed in the maximum slip of bond slip relationship between all samples exposed to 30 ^{0}C and 60 ^{0}C bond line temperatures. This indicates the initial softening of the bond with exposed temperature, does not depend on the thickness of the CFRP layer. At 90 ^{0}C bond line temperature, CFRP layer thickness shows a negligible effect on the bond slip relationship. Hence, it can be concluded that the bond-slip behavior mainly depends on the bond line properties and the thickness of adhesive layer.

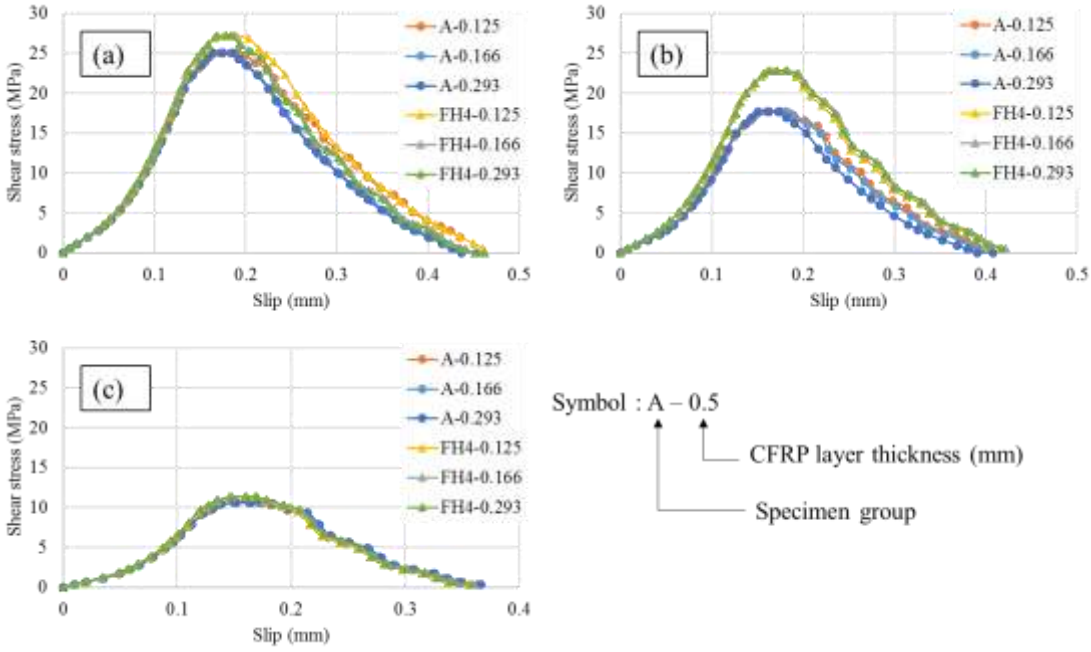

Figure 6.10 Effects of CFRP layer thickness on bond slip vs shear stress for bond line temperatures, (a) 30 ^{0}C (b) 60 ^{0}C (c) 90 ^{0}C

7. CONCLUSION

The current investigation on the bond performance of corroded steel/CFRP double strap joints has been carried out to evaluate the effects of CFRP bond length, level of corrosion and the surface preparation method. Relationship between bond shear stress and slip was also estimated with the varying surface roughness level. The numerical model developed to predict the CFRP/steel composite performance was able to validate the experimental results successfully which were obtained to determine the effective bond length of the CFRP/Steel joint. Even though the deviation between the experimental and numerical results was about 20% for the bond lengths less than 90 mm, it was about 5% for the bond lengths higher than 90 mm. In the experiments, the effective bond length was calculated to be 110 mm while FE model predicted a result between 110 mm and 120 mm. However, this ±5 mm deviation was negligible and effective bond length was determined to be 110 mm. Surface roughness properties of the steel plates with all four levels of corrosion; Corrosion levels A, B. C and D could be successfully simulated in the model. Simulation of the surface preparation method was assumed by changing the mechanical properties of the adhesive layer for each corrosion level. When both experimental and numerical results are analysed, surface preparation method 02 was identified to be having optimum surface roughness characteristics in the bonded joint. For the surface preparation method (02) maximum bond stress and respected slip was 33 MPa and 0.075 mm, respectively, while the surface preparation method (01) has shown values of 27 MPa and 0.1mm. According to the results obtained, the bond slip model is mostly dependent on the method of surface preparation, but not much on the level of corrosion. The highest initial slip and the maximum slip were encountered from the CFRP / steel joints of which the surfaces were prepared with Method (01).

Steel/epoxy/CFRP double strap joints were prepared at six different initial elevated temperature curing conditions. The bond strength was determined under the elevated environmental temperature exposure. The mechanical properties and glass transition temperatures of the bond were evaluated. The failure modes of CFRP/steel double strap joints were shifted from CFRP fiber rupture to CFRP/steel interface debonding with the transient elevated heat condition of the bond line. Failure loads were directly influenced by the bond line temperature and about 70% of strength reduction was noted when the bond line temperature reaches T_g + 25 ^{0}C. The initial curing temperature of the joint directly influences on the mechanical properties of the bond. A high rate of bond degradation appears when the bond line reaches the range of temperatures between 55 ^{0}C and 80 ^{0}C, i.e. T_g ^{0}C and T_g + 25 ^{0}C. When the bond line temperature reaches 90 ^{0}C (T_g + 35 ^{0}C), the retained bond properties were almost similar irrespective from the curing time and curing conditions. On average, 16% difference was noted between the glass transition temperature (T_g) of the bond

and pure epoxy adhesive. By increasing the curing temperature from 30 ^{0}C to 55 ^{0}C and 75 ^{0}C, T_g increases about 10% between each category. Curing time influences significantly on T_g when compared to the curing temperature. With increasing curing time from 1 hour to 4 hours, T_g increases on average from 10% to 20%. Ultimate strain of the bond increases about 50% with elevated temperature curing within the considered range. When the bond line exposes to the elevated temperature, the properties such as elastic modulus, Poisson's ratio, bond strength decreases in a similar manner. Degradation of mechanical properties was appeared when the bond line exposes to the temperature T_g – 10 ^{0}C. A flood light system with suitable capacity can be used for elevated temperature curing of CFRP strengthened steel members. It is quite safe to use the bond characteristics of samples tested in the control environment as an indication of practical performance. It is important to measure the material properties for applications rather than relying on the manufacturer provided properties because of the noted huge discrepancy between two figures.

A detailed numerical model was developed to simulate the bond characteristics of CFRP/steel joints cued at different conditions and their behavior with elevated environmental temperature exposure. FE model was successfully developed using test results from experimental programme. FE modelling using adhesive property degradation has predicted the failure loads to achieve a 1.087 correlation value. The assumption of neglecting the variation of steel and CFRP mechanical properties with the bond line temperature has not significantly affected the FEA predicted results. Strain variation of bond in experimental data and FEA predicted data had good agreement. However, end of the elastic region for bond was observed at 11 kN load for experimental results, while it was at 6 kN load for FEA predicted data. In the elastic region the FEA predicted strain readings were low compared to the experimental results. However, in the plastic region FEA predicted strain reading have shown higher values compared to experimental results. Bond line temperature of CFRP steel double strap joints has considerable effect on maximum shear stress in bond slip relationship. On average 60% reduction of maximum shear stress was observed when the bond line temperature increases from 30 ^{0}C to 100 ^{0}C. Initial slip and maximum slip also followed same reduction pattern with 17% and 25%, respectively. With increasing the initial curing temperature (up to 75 ^{0}C) and period (up to 4 hours) initial slip, maximum slip and maximum shear stress increases by 5%, 9% and 10% at bond line temperature 30 ^{0}C. However, 12%, 17% and 47% increase in initial slip, maximum slip and maximum shear stress has observed at 100 ^{0}C bond line temperature. Adhesive layer thickness has considerable effect on bond lip relationship for initial slip and maximum slip. On average 130% and 200% increase was observed for maximum slip and initial slip, when the adhesive layer thickness increases from 0.5 mm to 2.0 mm. However, maximum shear stress was

only affected by the curing condition. CFRP fabric type and thickness has negligible effect on bond slip relationship for almost every7 aspect. Maximum slip has decreased by 4% when the CFRP fabric type changes to UHM from GP and HM.

Acknowledgements

Funding provided by The Senate Research Committee, University of Moratuwa is highly appreciated (Grant No: SRC/LT/2016/19).

References

Nguyen, T. et al. (2013) 'Curing effects on steel / CFRP double strap joints under combined mechanical load, temperature and humidity', Construction and Building Materials. Elsevier Ltd, 40, pp. 899–907. doi: 10.1016/j.conbuildmat.2012.11.035.

Elchalakani, M., Karrech, A., Basarir, H., Zhaob, X., Fawzia, S. and Hassanein, M.F. (2017) 'Strengthening of mild steel struts using CFRP sheets subjected to uniform axial compression', Thin Walled Structures. Elsevier Ltd, 116(January), pp. 96–112. doi: 10.1016/j.tws.2017.03.010.

Colombi, P. and Fava, G. (2016) 'Fatigue crack growth in steel beams strengthened by CFRP strips', THEORETICAL AND APPLIED FRACTURE MECHANIC. Elsevier Ltd. doi: 10.1016/j.tafmec.2016.01.007.

Liu, M. and Dawood, M. (2017) 'Reliability analysis of adhesively bonded CFRP-to-steel double lap shear joint with thin outer adherends', Construction and Building Materials. Elsevier Ltd, 141, pp. 52–63. doi: 10.1016/j.conbuildmat.2017.02.113.

Selvaraj, S. and Madhavan, M. (2016) 'Enhancing the structural performance of steel channel sections by CFRP strengthening', Thin-Walled Structures, 108, pp. 109–121.

Elchalakani, M. (2016) 'Rehabilitation of corroded steel CHS under combined bending and bearing using CFRP', Journal of Constructional Steel Research. Elsevier Ltd, 125, pp. 26–42. doi: 10.1016/j.jcsr.2016.06.008.

Batuwitage, C. et al. (2017) 'Evaluation of bond properties of degraded CFRP-strengthened double strap joints', Composite Structures. Elsevier Ltd, 173, pp. 144–155. doi: 10.1016/j.compstruct.2017.04.015.

Al-mosawe, A., Kalfat, R. and Al-mahaidi, R. (2016) 'Strength of Cfrp-steel double strap joints under impact loads using genetic programming', *Composite Structures*. Elsevier Ltd. doi: 10.1016/j.compstruct.2016.11.016.

Yu, Q. Q. et al. (2016) 'Boundary element analysis of edge cracked steel plates strengthened by CFRP laminates', Thin-Walled Structures, 100, pp. 147–157. doi: 10.1016/j.tws.2015.12.016.

Ghaemdoust, M. R., Narmashiri, K. and Yousefi, O. (2016) 'Structural behaviors of deficient steel SHS short columns strengthened using CFRP', Construction and Building Materials. Elsevier Ltd, 126, pp. 1002–1011. doi: 10.1016/j.conbuildmat.2016.09.099.

Wang, Z. and Wang, Q. (2017) 'Fatigue behaviour of CFRP strengthened open-hole steel plates', Thin Walled Structures. Elsevier Ltd, 115(February), pp. 176–187. doi: 10.1016/j.tws.2017.02.015.

Al-zubaidy, H., Al-mahaidi, R. and Zhao, X. (2013) 'Finite element modelling of CFRP / steel double strap joints subjected to dynamic tensile loadings', Composite Structures, 99, pp. 48–61. doi: 10.1016/j.compstruct.2012.12.003.

Yue, Q. et al. (2016) 'Research on fatigue performance of CFRP reinforced steel crane girder', Composite Structures. Elsevier Ltd, 154, pp. 277–285. doi: 10.1016/j.compstruct.2016.07.066.

Focacci, F., Nanni, A. and Bakis, C.E. (2000) 'Local bond–slip relationship for FRP reinforcement in concrete', J Compos Construct ASCE, 4(1), pp.24–31

Lu, X.Z., Teng, J.G., Ye, L.P. and Jiang, J.J. (2005) 'Bond–slip models for FRP sheets/plates bonded to concrete', Eng Struct, 27(6), pp.920–37.

Dong, K. and Hu, K. (2016) 'Development of bond strength model for CFRP-to-concrete joints at high temperatures', Composites Part B. Elsevier Ltd, 95, pp. 264–271. doi: 10.1016/j.compositesb.2016.03.088.

Fawzia, S., Zhao, X. and Al-mahaidi, R. (2010) 'Bond – slip models for double strap joints strengthened by CFRP', Composite Structures. Elsevier Ltd, 92(9), pp. 2137–2145. doi: 10.1016/j.compstruct.2009.09.042.

Wang, R., Zheng, S. and Zheng, Y. (2011) 'Polymer matrix composites and technology', Woodhead Publishing Limited and Science Press Limited, pp.101-167

Gilbert, M. (2017) 'Brydson's Plastics Materials', Butterworth-Heinemann is an imprint of Elsevier, pp.59-73.

Carbas, R. J. C., Marques, E. A. S. and Marques, E. A. S. (2014) 'Effect of Cure Temperature on the Glass Transition Temperature and Mechanical Properties of Epoxy Adhesives', The Journal of Adhesion. 90, pp. 37–41. doi: 10.1080/00218464.2013.779559.

Rudin, A. and Choi, P. (2013) 'The Elements of Polymer Science & Engineering', Academic Press is an imprint of Elsevier, pp.149-229.

Kotynia, R., Adamczewska, K., Strakowska, A., Maslowski, M. and Strzelec, K. (2017) 'Effect of accelerated curing conditions on shear strength and glass

transition temperature of epoxy adhesives', 193, pp. 423–430. doi: 10.1016/j.proeng.2017.06.233.

Zhang, Y., Adams, R. D. and Lucas, F. M. (2014) 'Absorption and glass transition temperature of adhesives exposed to water and toluene', International Journal of Adhesion and Adhesives. Elsevier, 50, pp. 85–92. doi: 10.1016/j.ijadhadh.2014.01.022.

Nguyen, T. et al. (2011) 'Mechanical characterization of steel / CFRP double strap joints at elevated temperatures', Composite Structures. Elsevier Ltd, 93(6), pp. 1604–1612. doi: 10.1016/j.compstruct.2011.01.010.

Agarwal, A., Foster, S. J. and Hamed, E. (2016) 'Testing of new adhesive and CFRP laminate for steel-CFRP joints under sustained loading and temperature cycles', Composites Part B, 99, pp. 235–247.

Technical data sheet, ARELDITE 420 A/B, two component epoxy adhesive system, Huntsman Advanced Materials, Available at: http://.huntsman.com [Accessed 12 Aug. 2018].

Gilbert M. Brydson's Plastics Materials, Butterworth-Heinemann is an imprint of Elsevier. 2017, pp. 59-73.

Gamage JCPH, Al-mahaidi R, Wong MB. Integrity of CFRP-concrete bond subjected to longterm cyclic temperature and mechanical stress. Compos Struct2016;149:423–33. doi:10.1016/j.compstruct.2016.04.040.

Gamage JCPH, Wong B, Al-Mahaidi R. Performance of CFRP strengthened concrete members under elevated temperatures. In: International symposium on bond behaviour of FRP in structures (BBFS), Hong Kong. p. 7–9.

Gamage JCPH, Al-mahaidi R, Wong B, Ariyachandra MREF. Bond characteristics of CFRPstrengthened concrete members subjected to cyclic temperature and mechanical stress at low humidity. Compos Struct2017;160:1051–9. doi:10.1016/j.compstruct.2016.10.131.

Wang R, Zheng S, Zheng Y. Polymer matrix composites and technology, Woodhead Publishing Limited and Science Press Limited, 2011, pp.101-167.

Gamage JCPH, Al-mahaidi R, Wong B, Ariyachandra MREF. Bond characteristics of CFRPstrengthened concrete members subjected to cyclic temperature and mechanical stress at low humidity. Compos Struct2017;160:1051–9. doi:10.1016/j.compstruct.2016.10.131.

Ranasinghe RATM, Jinadasa DVLR, Srilal HPS, Gamage JCPH. Bond performance of cfrp strengthened concrete subjected to fire. In: Civil Engineering Research for Industry – 2011, Sri Lanka. p. 37-42.

Petrie, EM. Handbook of Adhesives and Sealants. McGraw-Hill Handbooks, 2006.

ANSYS mechanical user's guide, (2013) ANSYS, Inc. from http://www.ansys.com

Gamage JCPH, Wong MB. Bond characteristics of CFRP plated concrete members under elevated temperatures 2006;75:199–205. doi:10.1016/j.compstruct.2006.04.068.

Technical data sheet, X-Wrap C230, High strength carbon fiber fabric for structural strengthening, X-CALIBUR structural systems, Available at: http://.x-calibur.us [Accessed 12 Aug. 2018].

Technical data sheet, X-Wrap C530, High strength carbon fiber fabric for structural strengthening, X-CALIBUR structural systems, Available at: http://.x-calibur.us [Accessed 12 Aug. 2018].

Technical data sheet, X-Wrap C300, High strength carbon fiber fabric for structural strengthening, X-CALIBUR structural systems, Available at: http://.x-calibur.us [Accessed 12 Aug. 2018].

Appendices

Appendix A

List of publications appeared in appendix A in order,

1. Mechanical characterization of CFRP/steel bond cured and tested at elevated temperature – Composite Structures – Published
2. Numerical modelling of bond shear stress slip behavior of CFRP/steel composites cured and tested at elevated temperature – Composite Structures – Under review
3. Effects of elevated temperature curing on glass transition temperature of steel/CFRP joint and pure epoxy adhesive – Electronic Journal of Structural Engineering (EJSE) – Under review
4. Bond slip models for corroded steel/CFRP double strap joints - 6th International Symposium on Advances in Civil and Environmental Engineering Practices for Sustainable Development (ACEPS-2018) – Published
5. Fire performance of CFRP strengthened steel I beams cured at elevated temperature - The 9th International Conference on Sustainable Built Environment 2018 (ICSBE) - Submitted